VACCINES

An oral norovirus vaccine generates mucosal immunity and reduces viral shedding in a phase 2 placebo-controlled challenge study

Becca A. Flitter[1]*†, Joshua Gillard[2]†, Susan N. Greco[1]†, Maria D. Apkarian[1], Nick P. D'Amato[1], Lam Quynh Nguyen[1], Elena D. Neuhaus[1], Darreann Carmela M. Hailey[1], Marcela F. Pasetti[3], Mallory Shriver[3], Christina Quigley[4], Robert W. Frenck Jr.[4], Lisa C. Lindesmith[5], Ralph S. Baric[5], Lee-Jen Wei[6], Sean N. Tucker[1], James F. Cummings[1]*

There are currently no licensed vaccines for norovirus, a leading cause of epidemic and endemic gastroenteritis worldwide. Clinical advancement of promising vaccine candidates from phase 2 studies to phase 3 field trials has been hampered by the lack of robust immunological correlates of protection. Here, we conducted a phase 2b randomized, placebo-controlled vaccination and challenge study to assess the safety, efficacy, immunogenicity, and correlates of protection of VXA-G1.1-NN, an oral tablet norovirus vaccine. VXA-G1.1-NN was safe and well tolerated, conferred protection against norovirus GI.1 challenge, and reduced viral shedding in stool and emesis. Norovirus VP1-specific serum immunoglobulin A (IgA), IgG, and functional blocking antibody titers increased substantially after oral vaccination. Moreover, oral immunization stimulated VP1-specific IgA antibodies in nasal lining fluid, saliva, and fecal samples. Serum and mucosal antibody responses 7 days after vaccination were correlated with the induction of antibody-secreting, $\alpha4\beta7^+$ mucosal-homing B cells. Machine learning analyses of vaccine-stimulated immune components identified serum functional blocking antibody and fecal IgA as robust correlates of protection. These results demonstrate the potential of VXA-G1.1-NN as a safe and effective oral norovirus vaccine and reveal critical immunological features underpinning vaccine efficacy.

INTRODUCTION

Noroviruses (NVs) are a leading cause of epidemics, outbreaks, and sporadic cases of acute gastroenteritis (AGE) worldwide (*1*, *2*). Symptoms of infection include severe vomiting, diarrhea, and abdominal cramps that appear within 10 to 51 hours after exposure and last 2 to 4 days (*2*). Overall, 10% of people with NV-related AGE seek medical care that can include hospitalization and intravenous rehydration, with severe NV infections being more common in children and older adults (*3*). NVs are highly infectious and are transmitted by the fecal-oral route through waterborne, foodborne, and person-to-person pathways, as well as through aerosolized virus from emesis or poor sanitation (*4*, *5*). Viral shedding can precede the onset of illness and persist for weeks thereafter (*6*, *7*). Transmission often occurs in semiclosed environments, such as schools, nursing homes, hospitals, military bases, and child care centers (*8*). Consequently, controlling NV remains a major public health priority.

There are no licensed vaccines available to prevent NV infection. One NV vaccine candidate under development uses cell culture–based expression of NV capsid protein VP1, which spontaneously forms a virus-like particle (VLP). These VLPs have been combined with adjuvants to improve immunogenicity and can be administered orally, intranasally, and intramuscularly (*9*). Safety and immunogenicity of VLP-based vaccines have been demonstrated in younger adults (*10*–*13*), older adults (*14*), and children (*15*). Intranasal administration of an NV VLP vaccine (GI.1 genotype) reduced AGE in a human challenge study; however, this approach was not further developed (*16*). In a subsequent study, an intramuscular bivalent vaccine (targeting the GI.1 and 3 GII.4 NV genotypes) decreased illness severity after GII.4 challenge but did not reduce the incidence of AGE and NV infection, despite stimulating higher serum immunoglobulin G (IgG) and NV-blocking titers compared with intranasal vaccination (*17*). Because NV infects mucosal surfaces, vaccination through a mucosal route, as opposed to parenteral administration, may provide superior barrier immunity and enhance protection against NV infection (*18*, *19*). We have developed an oral tablet NV vaccine that has demonstrated immunogenicity in adults aged 18 to 80 years and generated strong systemic and mucosal immune responses at multiple barrier surfaces (*20*, *21*).

We have previously demonstrated that this oral vaccination approach uniquely affects disease and infection in an H1N1 influenza phase 2 challenge study (*22*). The efficacy of oral influenza vaccine candidate VXA-A1.1 was compared with that of the licensed injectable vaccine Fluzone. Although VXA-A1.1 resulted in hemagglutinin serum antibody responses roughly one-sixth the magnitude of those induced by Fluzone, efficacy between the two vaccines was equivalent (47% relative protection against infection of VXA-A1.1 versus 43% of Fluzone). Subsequent machine learning analyses identified key features of protective immunity underpinning the protection afforded by each vaccine, hemagglutinin-specific IgA antibody-secreting cells (ASCs) for VXA-A1.1 and serum hemagglutination-inhibition titers for Fluzone.

[1]Vaxart Inc., South San Francisco, CA 94080, USA. [2]Department of Medicine, Division of Cardiovascular Medicine, Stanford University School of Medicine, Stanford, CA 94305, USA. [3]Center for Vaccine Development, University of Maryland Baltimore School of Medicine, Baltimore, MD 21201, USA. [4]Division of Infectious Diseases, Cincinnati Children's Hospital Medical Center, Cincinnati, OH 45229, USA. [5]Department of Epidemiology, University of North Carolina, Chapel Hill, NC 27599, USA. [6]Harvard T.H. Chan School of Public Health, Harvard University, Boston, MA 02115, USA.
†These authors contributed equally to this work.
*Corresponding author. Email: bflitter@vaxart.com (B.A.F.); jcummings@vaxart.com (J.F.C.)

As NV vaccine development progresses from early-stage clinical evaluation to larger field trials for licensure applications, identifying robust correlates of protection (CoPs) against NV infection and disease is becoming increasingly important. Although efficacy is typically established on the basis of the ability of the vaccine candidate to prevent infection or disease, the ability to predict efficacy on the basis of established CoPs could substantially expedite vaccine development. Furthermore, CoPs may provide insight into the mechanistic basis of vaccine efficacy, informing vaccine design and subsequent studies (*23*). Preexposure saliva, serum, and fecal IgA concentrations; memory B cell abundance; and serum NV-blocking titers have all been correlated with protection (*7*, *16*, *23*–*28*), but the precise markers that can firmly predict protection against NV infection remain unresolved.

In this study, we report the safety, immunogenicity, efficacy, and CoPs of VXA-G1.1-NN, an oral tablet NV vaccine. VXA-G1.1-NN comprises a nonreplicating adenovirus–based vector expressing the VP1 gene from the NV GI.1 genogroup and a double-stranded RNA adjuvant specifically designed to enhance expression in the intestine (*21*). These results demonstrate the potential of VXA-G1.1-NN as an effective oral NV vaccine and reveal immunological features underpinning the efficacy of this tablet delivery approach.

RESULTS

Recruitment and study design

We conducted a single-center double-blind study at AltaSciences LA (Cypress, CA) between January 2022 and April 2023 to evaluate the safety, immunogenicity, efficacy, and CoPs of oral vaccination with VXA-G1.1-NN in healthy adult volunteers. Overall, 523 individuals were screened against a set of inclusion and exclusion criteria, and in total, 165 individuals (18 to 49 years of age) were enrolled and randomly assigned 1:1 to receive VXA-G1.1-NN ($n = 86$) or placebo ($n = 79$). A total of 24 participants (VXA, $n = 10$; placebo, $n = 14$) discontinued the study after the vaccination phase. Of these, five were excluded for medical reasons (back pain, infection, or investigator discretion for safety). The remaining 19 nonchallenged participants recruited as backups were either not required to return (maximum number of participants in the challenge unit was limited to 12) or elected not to return. In the challenge phase, participants received an oral challenge inoculum of GI.1 NV 28 days after vaccination (VXA, $n = 76$; placebo, $n = 65$) (Fig. 1A). Because of scheduling conflicts, 21 of the 141 received the inoculum with the next cohort, at most 56 days postvaccination. Baseline demographic characteristics were similar between study groups in the vaccine and challenge phases (table S1).

Participants moved sequentially through the study phases of enrollment and vaccination [spanning D1 (day 1) to D28] to NV challenge spanning up to 8 days in the challenge unit [C1 (challenge day 1) to C8; Fig. 1B]. In the challenge phase, participants were monitored for signs and symptoms of AGE from C1 until discharge on C5 if symptoms subsided or up to C8 if symptoms persisted, according to the judgement of the investigator. Emesis and stool samples were collected and analyzed with quantitative reverse transcriptase polymerase chain reaction (qPCR) to quantify viral shedding in stool and emesis (Fig. 1B).

Immunogenicity end points were assessed on D1 (prevaccination baseline), D8, D28, and C29 (29 days postchallenge) (Fig. 1B). GI.1 VP1–specific IgA and IgG antibody concentrations in serum and IgA in nasal lining fluid (NLF), saliva, and fecal extracts were measured with Meso Scale Discovery immunoassay or enzyme-linked immunosorbent assay. In addition, the functional capacity of serum samples was assessed by NV–blocking antibody assay (NBAA) where the inhibition of GI.1 VLP binding to the Lewis b (Le^b) histoblood group antigen (HBGA) was quantified (*21*). IgA ASCs and frequencies of mucosal-homing B cells were measured from circulating peripheral blood mononuclear cells (PBMCs) collected 1 week after vaccine administration (*29*, *30*).

VXA-G1.1-NN is safe and well tolerated after NV challenge

No vaccine-related serious events or dose-limiting toxicities were reported. Within the first 7 days after vaccination, 58.1% of participants in the VXA-G1.1-NN group and 45.6% of participants in the placebo group reported solicited adverse events (AEs). Most events were mild, with few moderate and no severe events reported (table S2). Overall, the most common solicited AEs postvaccination were malaise and fatigue, reported by a similar proportion of participants who received VXA-G1.1-NN [29.1% (25 of 86)] or placebo [25.3% (20 of 79)], and headache, also reported by a similar proportion of VXA-G1.1-NN recipients [29.1% (25 of 86)] and placebo recipients [24.1% (19 of 79)]. Diarrhea was reported in 19.4% of the participants: 23.3% in the VXA-G1.1-NN group and 15.2% in the placebo group; these were mostly of mild severity, with several moderate and no severe cases (table S2). Through D28, unsolicited AEs occurred in 8.1% (7 of 86) of participants who received VXA-G1.1-NN and 11.4% (9 of 79) of those who received placebo (table S3). Vaccine-related unsolicited AEs occurred in 3.5% (3 of 86) of VXA-G1.1-NN recipients and 3.8% (3 of 79) of placebo recipients. The vaccine-related events in the VXA-G1.1-NN group were diarrhea, fatigue, malaise, and decreased appetite. Vaccine-related events in the placebo group were nausea, fatigue, and decreased appetite. All vaccine-related events were mild in severity. No vaccine-related notable clinical laboratory or electrocardiogram abnormalities were reported. Together, VXA-G1.1-NN was well tolerated, with a favorable safety profile showing no serious vaccine-related AEs.

During the challenge phase, at least one solicited NV symptom was reported in 77.6% of VXA-G1.1-NN participants and 84.6% of placebo participants. Symptoms in both groups were mostly mild or moderate, with 11.8% (9 of 76) of VXA-G1.1-NN participants and 18.5% (12 of 65) of placebo participants reporting severe solicited NV symptoms. Nausea was reported in 50% (38 of 76) and emesis in 36% (28 of 76) of the VXA-G1.1-VXA group, whereas in the placebo cohort, 59% (38 of 65) experienced nausea and 50% (33 of 65) experienced vomiting (table S2). Abdominal cramps and pain were reported in 42% (32 of 76) of the VXA-G1.1-VXA cohort and 60% (39 of 76) of the placebo cohort. Fever was reported in 5.3% (4 of 76) of the VXA-G1.1-NN group and 6.2% (4 of 65) of the placebo group. Other solicited symptoms, including myalgia, abdominal cramps or pain, and abdominal gurgling or bloating, were similar between groups. In addition, 21.1% (16 of 76) of participants who received VXA-G1.1-NN and 23.1% (15 of 65) of placebo participants reported unsolicited AEs related to NV challenge, all of mild severity. Overall, headache was the most common unsolicited AE during the challenge phase and was experienced by a similar proportion of participants in both groups (VXA-G1.1-NN: 26.3%, 20 of 76 participants; placebo: 24.6%, 16 of 65 participants) (table S3). One participant in the VXA-G1.1-NN group experienced an AE of mild tachycardia that occurred 2 days postchallenge and was considered related to challenge.

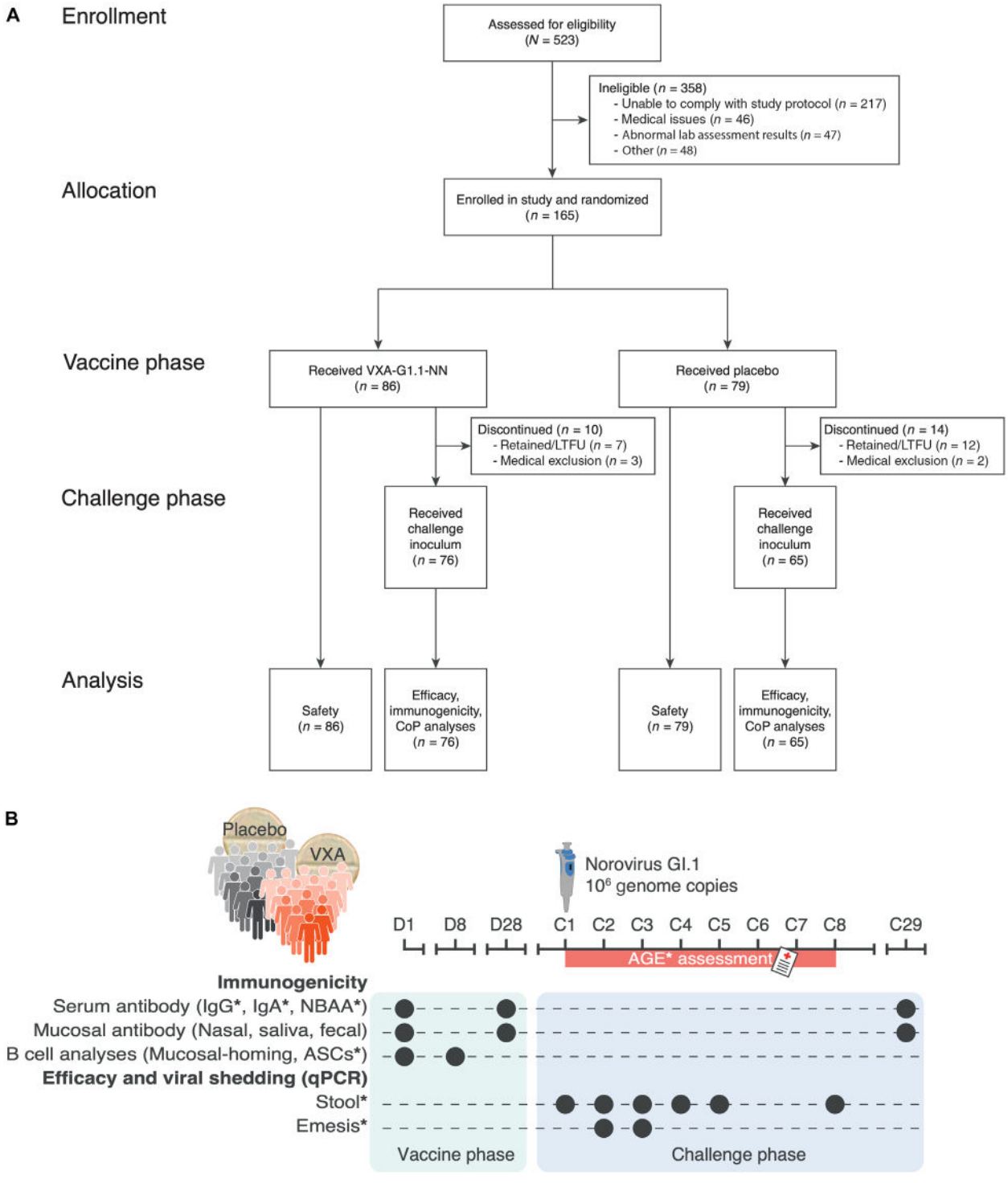

Fig. 1. Flow diagram and study procedures. (**A**) Flow diagram of participants who were enrolled and analyzed in a phase 2b double-blind, single-site randomized human challenge trial. On D1, participants received one oral dose of VXA-G1.1-NN or placebo (vaccine phase) and were subsequently challenged with 10^6 genome copies of live NV GI.1 (challenge phase). (**B**) Study timeline indicating AGE assessment as well as immunogenicity and viral shedding analyses at each time point. An asterisk marks data assessed as prespecified primary end points. Vaccine and challenge phases of the study are indicated on the bottom margin. LTFU, lost to follow-up.

Other challenge-related events in the VXA-G1.1-NN group included chills (3.9%), gastroesophageal reflux (1.3%), and decreased appetite (1.3%), and events in the placebo group included chills (3.1%), decreased appetite (3.1%), back pain (1.5%), and dizziness (1.5%).

VXA-G1.1-NN protects against NV challenge and is immunogenic

The prespecified primary efficacy end point was the proportion of participants showing evidence of NV gastroenteritis, defined as

meeting one or more definitions for AGE and NV infection by qPCR (Fig. 2A). Among VXA-G1.1-NN recipients, 57.1% developed NV infection, compared with 81.5% in the placebo group, with a 23.6% difference [95% confidence interval (CI): 7.4 to 38.0%, $P = 0.003$] and 30% relative reduction. NV gastroenteritis in the VXA group was 44.7% compared with 56.9% in the placebo group, although the difference of 12.2% (95% CI: −4.24 to 28.61%, $P = 0.178$) and relative reduction of 21% were not statistically significant (Fig. 2A and fig. S1, A and B). A sensitivity analysis that excluded 21 participants challenged later than 29 days postvaccination demonstrated vaccine efficacy equivalent to that in the full cohort (fig. S1C).

Vaccination with VXA-G1.1-NN significantly increased serum VP1-specific IgA, IgG, and NBAA titer end points on D28 and ASCs compared with placebo on D8 ($P < 0.0001$ for all prespecified primary end points; Fig. 2A and fig. S1, D to G). There were no statistically significant differences between groups in the prevaccination serum VP1-specific IgA, IgG, or NBAA concentrations (all $P > 0.05$). In the VXA group, on D28 postvaccination, GI.1-specific serum IgA and IgG concentrations were 8.76-fold (95% CI: 5.18 to 14.81) and 5.68-fold (95% CI: 3.67 to 8.79) higher than placebo, respectively, and blocking titers by NBAA were 4.09-fold (95% CI: 2.83 to 5.92) higher. Corresponding geometric mean fold rises (GMFRs) over D1 in the VXA-G1.1-NN group were 7.22 (95% CI: 5.24 to 9.94) for IgA, 4.65 (95% CI: 3.67 to 5.89) for IgG, and 4.06 (95% CI: 3.2 to 5.14) for NBAA titers at each time point (table S4). Antibody responses in the VXA group were accompanied by an increase in circulating ASCs of 364.59 (95% CI: 242.31 to 486.87) counts per 10^6 PBMCs compared with placebo (Fig. 2A).

In addition to evaluating the immunogenicity and efficacy of VXA-G1.1-NN through the prespecified primary end points, we quantified the totality of evidence supporting a beneficial vaccine effect by considering the probability of observing multiple simultaneous positive outcomes with statistical meta-analysis (*31*, *32*). Briefly, test statistics for each primary end point were calculated (Fig. 2A, right margin), and the mean test statistic value was obtained (mean test statistic, 5.66). Thereafter, group assignment was permuted, and the mean test statistic was recalculated for each of 10,000 iterations, generating a distribution of scores representing the null hypothesis that there is no vaccine effect (Fig. 2B). The probability of the observed mean test statistic was $P < 0.0001$, indicating an overall significant beneficial effect of VXA-G1.1-NN. These findings highlight the overall efficacy of VXA-G1.1-NN, prompting further characterization of the underlying infection dynamics and mechanisms driving vaccine effectiveness.

VXA-G1.1-NN reduces viral shedding in stool and emesis and modulates humoral immune responses to NV infection

We also examined a set of exploratory end points to further quantify different characteristics of vaccine efficacy. The overall rate of AGE (fig. S2A) and the severity of gastroenteritis by the modified Vesikari score (*33*) were similar between groups (fig. S2B). However, the proportion of participants who displayed neither qPCR-detectable NV infection nor AGE symptoms ($qPCR^-$, AGE^-), representing an important group that resisted the challenge, was significantly higher in the VXA group (34.2% versus 15.3%, $P = 0.012$), corresponding to an 18.8% increase in resistant participants (95% CI: 4.9 to 34.2%; Fig. 3A).

Next, we examined emesis rates and viral loads in emesis and stool at specific days during the challenge period to characterize viral shedding dynamics. Emesis cases occurred within 2 to 3 days postchallenge (C2 and C3). On C3, the emesis rates were 26.3% in the VXA group and 40.0% in the placebo group ($P = 0.105$, Fig. 3B). Although the emesis rate was comparable between groups, the VXA group had significantly less detectable NV RNA in emesis samples at C2 ($P = 0.0276$, Fig. 3C). Similarly, stool samples showed significantly reduced viral RNA loads in the VXA group on C4 ($P = 0.0168$) and C8 ($P = 0.0009$) (Fig. 3D and fig. S2C). Given that overall AGE rates were comparable between study groups but that NV infection was reduced by vaccination, we assessed asymptomatic viral shedding. We observed that the proportion of $qPCR^+AGE^-$ participants was 13.1% in the VXA group and 24.6% in the placebo group ($P = 0.087$, Fig. 3E).

One of the drawbacks of assessing NV infection by qPCR is the difficulty in correlating genomic copies with infectious particles in a sample. NV GI.1 is extremely difficult to propagate in cell culture, and reliable methods for measuring infectious particles of GI.1 in stool have yet to be developed. Consequently, interpreting qPCR data alone may overestimate the number of infectious units in a sample (*34*). To address this, serological evidence as a measure of NV and other viral infections has been used in human challenge and vaccination studies analyzing immune responses to live infectious viruses (*35*–*37*). Therefore, we also examined seroconversion after NV challenge as an end point, defined as a greater than fourfold increase in VP1-specific serum IgG antibody from D28 (postvaccination, pre–NV

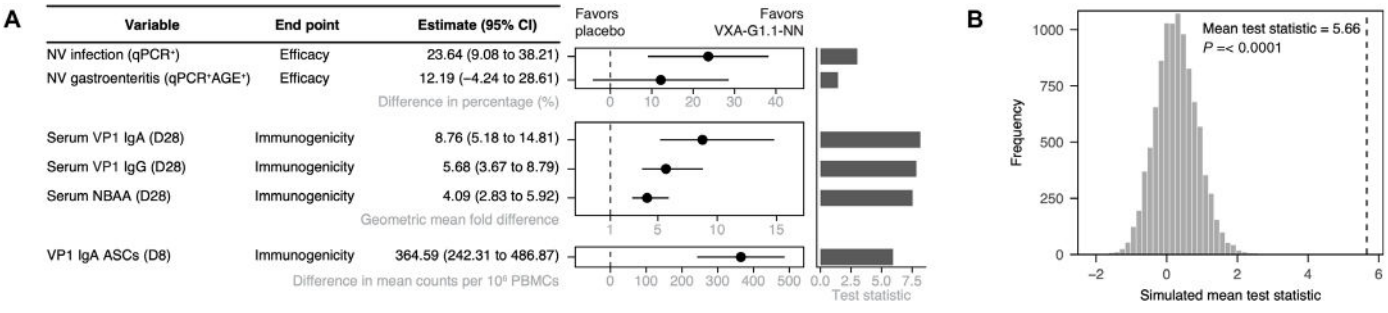

Fig. 2. VXA-G.1.1-NN is effective and immunogenic. (**A**) Table and forest plot of results for individual prespecified primary efficacy and immunogenicity end points. Estimates of the difference between placebo and VXA-G1.1-NN with 95% CIs shown with the associated test statistic. The two-sample proportion test or *t* test was used for efficacy or immunogenicity end points, respectively. (**B**) Histogram of simulated mean observed test statistic assuming no vaccination effect of VXA-G1.1-NN. The vertical line marks the mean observed test statistic, and the one-sided *P* value is shown. Data are shown for $n = 65$ (placebo) and $n = 76$ (VXA-G1.1-NN) participants.

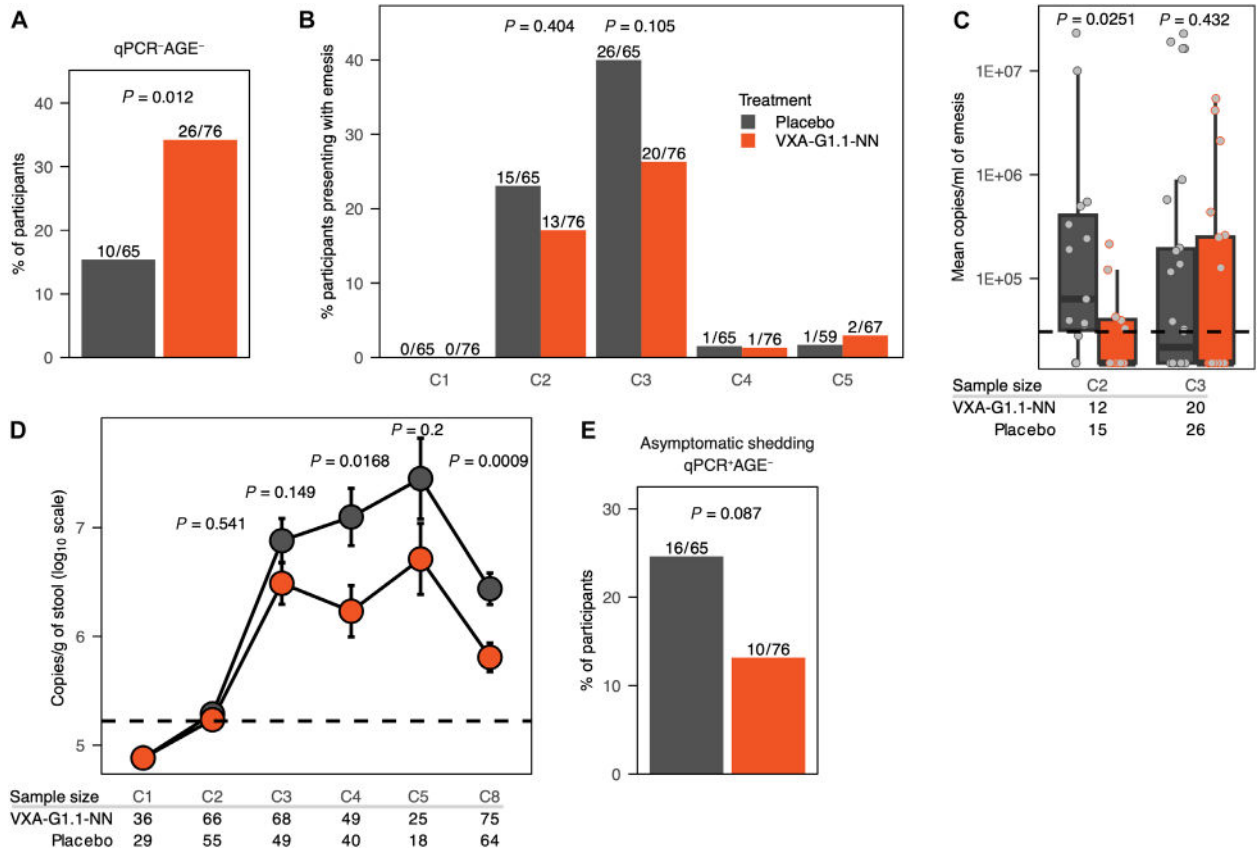

Fig. 3. VXA-G1.1-NN reduces viral shedding in stool and emesis. (**A**) Proportion of participants who did not present symptoms of AGE (AGE$^-$) and whose emesis and stool samples did not contain detectable genomic NV viral RNA (qPCR$^-$). (**B**) Proportion of participants in the VXA-G1.1-NN and placebo study groups presenting emesis on each of the indicated study days. (**C**) Genomic copies of viral RNA per milliliter of emesis of participants in each study group. Each data point corresponds to the geometric mean of emesis samples collected for each participant on each of the indicated study days. The dashed line indicates the limit of detection. Data are presented as box plots, with bounds from the 25th to 75th percentiles, median line, and whiskers, which extend to the largest or smallest value no further than 1.5 times the interquartile range. (**D**) Genomic copies of viral RNA per gram of stool. Data are presented as a point-line graph of the study group mean with standard error. For (C) and (D), the number of participants in each study group on each study day is indicated on the bottom margin. Two-sided Wilcoxon test and nominal *P* values are shown within the plots. (**E**) Proportion of participants who did not present symptoms of AGE (AGE$^-$) and whose emesis and stool samples contained detectable genomic NV viral RNA (qPCR$^+$). Data in (A) and (D) are presented as ratios of positive cases among the total study group, and differences in ratios between study groups were tested with two-sided Fisher's exact test.

challenge) to C29 (29 days post–NV challenge). The proportion of participants in the VXA group who seroconverted in this time frame was significantly lower than that in the placebo group (47.4% versus 81.5%, $P < 0.0001$) (fig. S2D).

VXA-G1.1-NN stimulates mucosal antibodies and mucosal-homing B cells

NV-specific saliva IgA is associated with clinical protection (*27*, *28*), and oral vaccination stimulates immune responses in the gastrointestinal tract and distal sites such as the respiratory and oral mucosa (*21*). We measured VP1-specific IgA antibody responses in fecal, NLF, and saliva samples as evidence of mucosal immune responses at these sites. To account for variations in IgA content because of sampling, we normalized VP1-specific IgA antibody values by the total IgA in each sample. As a first step toward characterizing immune dynamics induced by VXA-G1.1-NN vaccination and challenge with live NV, we visualized serum and mucosal antibody trends at baseline (D1), D28, and C29 (Fig. 4, A to C) and fitted a linear-mixed-effects regression model for each variable to compare antibody concentrations between VXA and placebo over time. Baseline antibody concentrations were not different between the placebo and VXA study groups. Compared with placebo, vaccination with VXA-G1.1-NN significantly increased VP1-specific IgA antibodies in fecal (GMFR = 4.25; 95% CI: 2.4 to 7.52, $P < 0.0001$), NLF (GMFR = 4.32; 95% CI: 3.05 to 6.11, $P < 0.0001$), and saliva samples (GMFR = 3.29; 95% CI: 2.35 to 4.6, $P < 0.0001$) by D28 (Fig. 4D). Corresponding GMFRs over D1 in the VXA-G1.1-NN group were 2.64 (95% CI: 1.61 to 4.33, $P < 0.0001$) in fecal, 3.62 (95% CI: 2.72 to 4.83, $P < 0.0001$) in NLF, and 2.9 (95% CI: 2.25 to 3.73, $P < 0.0001$) in saliva samples. Similar to serum antibody values, mucosal IgA values further increased in the VXA group after NV challenge by C29 and were not different compared to those of the placebo group (Fig. 4, A to C, and fig. S1, D to F). Geometric mean concentrations of mucosal antibody are presented in table S4. Overall, at each study time point, amounts of IgA antibodies in NLF, saliva, and fecal samples (Fig. 4, A to C) had dynamics similar to those of serum IgA, IgG, and NBAA responses (fig. S1, D to F). In line with this, baseline-normalized increases in serum antibody responses and NBAA were highly correlated with

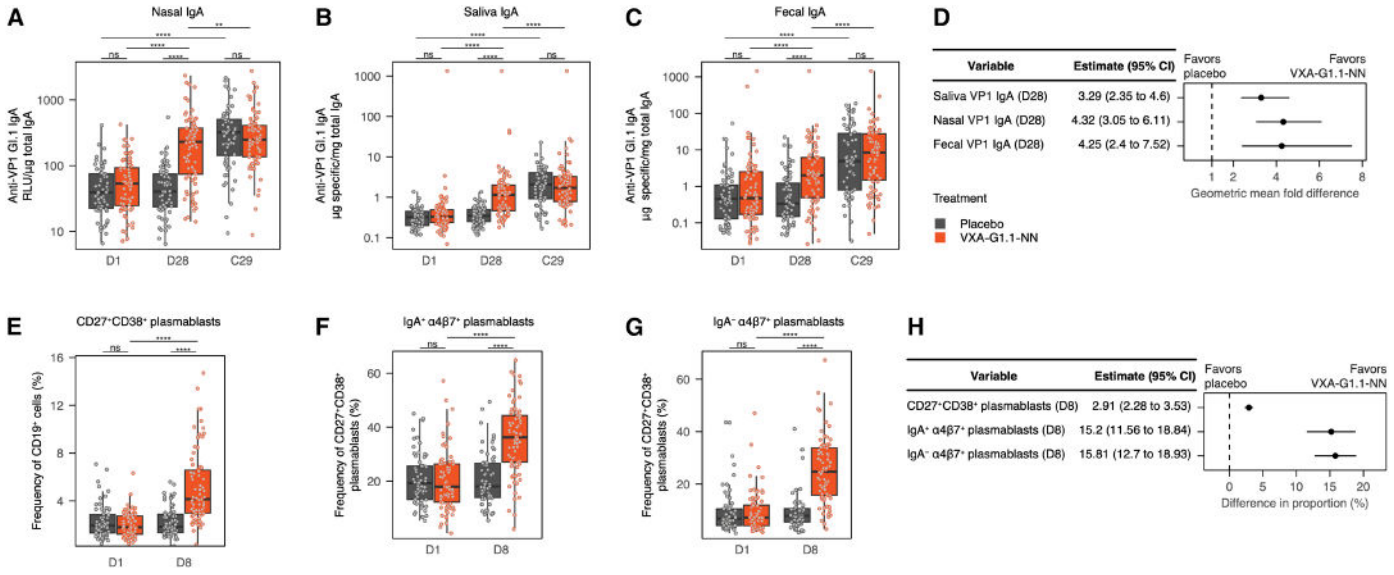

Fig. 4. VXA-G1.1-NN stimulates mucosal antibody responses and mucosal-homing plasmablasts. (**A** to **C**) VP1 IgA mucosal antibody concentrations in NLF (A), saliva (B), and fecal (C) samples are shown at the prevaccination baseline (D1), 27 days postvaccination (D28), and 29 days postchallenge (C29). Nominal VP1 antibody concentrations were normalized as a ratio of total IgA in each sample. Data are $n = 76$ for the VXA-G1.1-NN study groups and $n = 64$ or 65 for the placebo study groups. RLU, relative light units. (**D**) Table and forest plot of results for each mucosal antibody end point on D28. Estimates of the difference between placebo and VXA-G1.1-NN with 95% CIs are shown. (**E** to **G**) Frequencies of $CD27^+CD38^+$ plasmablasts among $CD19^+$ cells (E), frequencies of IgA^+ $a4\beta7^+$ plasmablasts among $CD27^+CD38^+$ cells (F), and frequencies of IgA^- $a4\beta7^+$ plasmablasts among $CD27^+CD38^+$ plasmablast cells (G) are shown at the baseline and 8 days postvaccination (D8). Data are $n = 65$ and $n = 76$ for the placebo and VXA-G1.1-NN study groups, respectively. (**H**) Table and forest plot of results for each plasmablast cell population on D8 and estimates of the difference between placebo and VXA-G1.1-NN with 95% CIs are shown. Data are presented on each study day for VXA-G1.1-NN and placebo study groups as box plots, with bounds from the 25th to 75th percentiles, median line, and whiskers, which extend to the largest or smallest value no further than 1.5 times the interquartile range. Points correspond to a sample from each participant. *P* values, estimates, and significance were calculated with a linear-mixed-effects model fitting each antibody measurement as the outcome and time, study group, and their interaction as main effects. Participant ID was fitted as a random effect. $^{**}P < 0.01$; $^{****}P < 0.0001$; ns, not significant.

those of NLF and saliva IgA responses, which were themselves also highly intercorrelated (Spearman's rho range, 0.47 to 0.68; fig. S3).

On D8, the VXA-G1.1-NN group had significantly increased ASCs in the peripheral blood such that 79.7% of participants had counts above the responder threshold of 23 spots per 10^6 PBMCs ($P < 0.0001$, fig. S1G). This transient increase in circulating plasmablasts and increased expression of antigen-specific $\alpha4\beta7^+$ plasmablasts have been investigated as a proxy marker of mucosal immune protection against orally delivered live attenuated vaccines (*29*). In previous studies, we have demonstrated a strong induction of $\alpha4\beta7^+$ mucosal-homing B cells in participants who were orally immunized with VXA-G1.1-NN (*21*). We therefore conducted PBMC immunophenotyping to quantify $\alpha4\beta7^+$ plasmablast responses on D8 (fig. S4A). Although frequencies of total $CD19^+$ B cells were comparable between study groups at each study time point and did not change in response to vaccination (fig. S4B), the frequency of plasmablast cells ($CD19^+$, $CD27^+$, and $CD38^+$) significantly increased by D8 in the VXA-G1.1-NN group ($P < 0.0001$, Fig. 4E). We further examined IgA^+ and IgA^- $\alpha4\beta7^+$ expression from $CD19^+$, $CD27^+$, and $CD38^+$ populations to quantify changes in plasmablast isotype and homing. By 8 days postvaccination, both IgA^+ and IgA^- $\alpha4\beta7^+$ plasmablast frequencies were significantly increased in the VXA-G1.1-NN group compared with both the prevaccination baseline ($P < 0.0001$, Fig. 4F; $P < 0.0001$, Fig. 4G) and placebo group (mean difference, 15.2% IgA^+ $\alpha4\beta7^+$, $P < 0.0001$, and 15.81% IgA^- $\alpha4\beta7^+$ plasmablasts, $P < 0.0001$, Fig. 4H). These increases were paired with a concomitant decrease in $\alpha4\beta7^-$ plasmablasts ($P < 0.0001$, fig. S4, C to E). We hypothesized that increases in VP1 IgA^+ circulating ASCs and $\alpha4\beta7^+$ plasmablasts were associated with subsequent increases in antigen-specific serum and mucosal antibody responses. To address this, we calculated pairwise correlations between baseline-normalized increases in these B cell populations and those in serum and mucosal antibodies (fig. S4F). ASC responses were highly correlated with serum and mucosal antibody responses. Increases in IgA^+ $\alpha4\beta7^+$ plasmablasts were most highly correlated with serum, saliva, and NLF IgA responses, whereas IgA^- $\alpha4\beta7^+$ plasmablasts were correlated with serum IgG and NBAA. Changes in IgA^- $\alpha4\beta7^+$ plasmablast frequency were also correlated with increases in fecal, NLF, and saliva IgA. Overall, our data show that a single oral vaccination of VXA-G1.1-NN stimulated elevated and antigen-specific immunity compared with placebo. These include increases in multiple systemic and mucosal immune features, including mucosal-homing B cells; IgA ASCs; NLF, saliva, and fecal IgA; serum IgG and IgA; and blocking antibodies. In addition, antibody responses in participants receiving VXA-G1.1-NN were correlated with the strong early induction of antigen-specific and mucosal-homing plasmablasts.

VP1-specific fecal IgA and serum blocking titer are CoPs against NV infection

We observed that the VXA-G1.1-NN vaccine protects against NV infection (Fig. 2A), reduces shedding (Fig. 3, B and C), and stimulates antibody-secreting mucosal-homing B cells with systemic and mucosal antibody responses (Fig. 4 and fig. S1G). We also found that serum IgG, serum IgA, NBAA, and fecal IgA abundance on

D28 correlated with the NV infection end point (fig. S5). These immune parameters were also intercorrelated with other immune variables, suggesting that a variety of immune components is associated with protection conferred by VXA-G1.1-NN. To determine whether a multivariable profile could predict whether vaccinated participants would become infected after NV challenge, we evaluated two machine learning algorithms, the least absolute shrinkage and selection operator (Lasso) (*38*) and random forest (*39*). Lasso and random forest models were trained with antibody and B cell data collected on D28 and D8, respectively (fig. S1, D to G; Fig. 4; and fig. S4, B to D), to predict NV infection class labels in the VXA-G1.1-NN study group (fig. S1A). We used a repeated train-test resampling approach in all modeling to prevent overfitting and to obtain an unbiased estimate of model performance on unseen samples. Model performance was assessed using a Wilcoxon test comparing prediction scores of NV infection classes, and model accuracy was calculated as the area under the receiver operating characteristic (ROC) curve (AUC) with 95% CIs. Variable importance scores indicating the relative contribution to model predictions are presented for each model.

Both Lasso and random forest models were highly predictive of NV infection in the VXA-G1.1-NN study group (Fig. 5). The highest predictivity was obtained from the Lasso model (Wilcoxon test of prediction scores, $P = 0.0000858$, AUC = 0.76, 0.64 to 0.88; Fig. 5, A and B). NBAA and fecal IgA values on D28 were highly important for model predictions (Fig. 5C). Random forest showed similarly high performance (Wilcoxon, $P = 0.000404$, AUC = 0.73, 0.62 to 0.85; Fig. 5, D and E). Like Lasso, NBAA and fecal IgA values were the top-contributing immune markers and were followed by serum IgG and IgA abundance and IgA^- $\alpha4\beta7^+$plasmablast frequency (Fig. 5F). Although serum IgG was weakly correlated with NV infection in the placebo cohort (fig. S5B), markers measured in the placebo study group did not predict NV infection with either the Lasso (Wilcoxon, $P = 0.472$, AUC = 0.57, 0.40 to 0.74) or random forest models (Wilcoxon, $P = 0.375$, AUC = 0.58, 0.39 to 0.78; fig. S6). Together, our data show

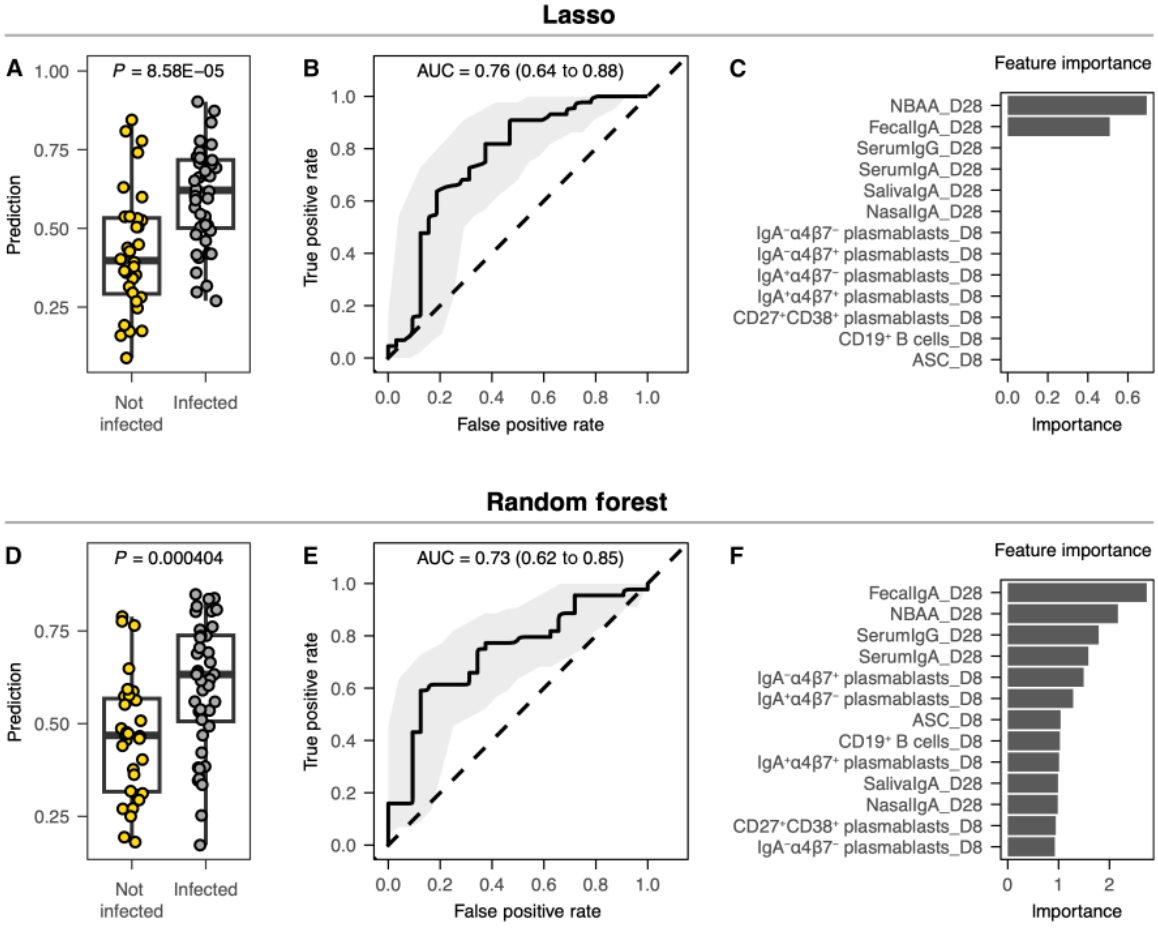

Fig. 5. Lasso and random forest models predict protection in VXA-G1.1-NN–vaccinated participants. Lasso and random forest prediction models were trained to predict whether a participant was infected using prechallenge immunogenicity data collected on D28 postvaccination with VXA-G1.1-NN. Infection was defined as the detection of NV RNA in at least one stool or emesis sample during the study period. (**A**) Prediction scores are shown for $n = 76$ participants in the VXA-G1.1-NN study group with the true outcome, infected ($n = 44$) or not infected ($n = 32$) (related to fig. S1A). (**B**) Prediction accuracy is shown with an ROC curve and corresponding AUC with 95% CIs. (**C**) Prechallenge immunogenicity features are shown with the corresponding importance score for model predictions. (**D** to **F**) Results of the random forest model are shown similarly to the Lasso model, including prediction scores (D), ROC curve and AUC (E), and feature importance scores (F). Data in (A) and (D) are presented as box plots, with bounds from the 25th to 75th percentiles, median line, and whiskers, which extend to the largest or smallest value no further than 1.5 times the interquartile range. Points correspond to a model prediction of each participant. Prediction scores between infection classes were compared with a two-tailed Wilcoxon test, and nominal *P* values are shown within the plot.

that protection conferred by VXA-G1.1-NN can be predicted by vaccine-stimulated immune markers, identifying NBAA and fecal IgA as robust CoPs against NV infection.

DISCUSSION

The extreme infectiousness and transmissibility of human NVs, coupled with the substantial morbidity associated with human NV infections, place a premium on the availability of a vaccine capable of preventing infection and limiting transmission (*40*). Despite this, there are currently no licensed vaccines for NV. Here, we show in a placebo-controlled challenge study that VXA-G1.1-NN, an orally administered NV vaccine, was well tolerated, conferred protection against NV challenge, and reduced viral shedding in stool and emesis. Consistent with our previous report, VXA-G1.1-NN immunization resulted in no vaccine-related serious or grade 3 solicited events (*21*). In the current study, vaccinated participants were protected against experimental challenge with NV with a 30% relative risk reduction for qPCR-detectable infection and a 21% relative risk reduction in NV gastroenteritis. The protection conferred by VXA-G1.1-NN was accompanied by increases in key immunogenicity parameters, including the induction of functional serum antibodies, mucosal IgA, ASCs, and circulating mucosal-homing plasmablasts. A totality of evidence analysis spanning primary end points further supported a beneficial effect of VXA-G1.1-NN vaccination. Subsequent machine learning analyses highlighted CoPs, with NBAA and fecal IgA predicting protection against NV challenge.

In addition to these protective effects, vaccination reduced fecal viral shedding for up to 1 week postchallenge and inhibited asymptomatic shedding (25% shedding in placebo and 13% in VXA-G1.1-NN). Given that fecal shedding can persist for up to 60 days after infection and that the magnitude and duration of shedding are comparable between asymptomatic and symptomatic cases (*41*), VXA-G1.1-NN may broadly reduce environmental viral spread. Shedding in emesis was also reduced as early as 1 day postchallenge, as was the frequency of emesis 2 days postchallenge. These results have important implications for NV transmission. Vomiting is a key route of transmission, as indicated by outbreak studies demonstrating that the risk of NV illness is correlated with both the number of and proximity to vomiting events (*42*–*44*). We hypothesize that vaccination likely affects transmission by reducing the amount of virus seeded into the environment through fomites and airborne droplets.

Immune CoPs can accelerate vaccine development by uncovering markers predictive of vaccine efficacy; such a tool can help identify promising early-stage candidates and facilitate evidence-based progression from late-stage trials to licensure (*45*). Defining CoPs for NV requires an understanding of mucosal immunity and its relationship to systemic immunity and vaccine effectiveness (*45*). The analysis of a set of 13 immune features (comprising previously reported CoPs and spanning multiple protective mechanisms, including mucosal antibodies, serum antibodies, and B cell immunity) revealed that these features were affected by vaccination and covaried with one another. In line with previous studies, univariable analyses identified correlations of serum IgG and IgA (*26*, *46*), fecal IgA (*7*), and HBGA–blocking antibody titers (*16*, *25*, *26*) with protection. Our study extends these data by providing evidence that fecal IgA and NBAA titers are sufficient to predict infection with high accuracy (AUC = 0.76, $P = 0.0000858$). One explanation for these results is that serum antibodies and other markers result from an overall increase in immune activation that is redundant and that functional, local IgA responses are critical for providing NV protection.

Mucosal vaccination may be central to stimulating this targeted response. A recent study initiated by Hillevax Inc. evaluated a bivalent injected vaccine in infants that induced substantial serum antibody responses (*47*) but failed to demonstrate efficacy (NCT05281094). Similarly, intramuscular vaccination of adults did not affect infection despite high HBGA-blocking titers (*17*, *26*). Two intranasal doses of VLP vaccine administered with chitosan and monophosphoryl lipid A adjuvants provided some protection against homologous GI.1 challenge (*16*). Intranasal VLP immunization elicited an increase in serum HBGA blocking antibody that was associated with a reduction in NV gastroenteritis; however, mucosal responses were not assessed. Although serum IgA increased after two doses of intranasal VLP immunization, it is not clear whether this route of administration stimulates fecal IgA responses, which we show here are critical for mediating protection against NV infection in gastrointestinal tissues. Considering that blocking titers were loosely correlated with protection after infection, an important conclusion from our study and the breadth of published work is that vaccine-stimulated NV CoPs are tightly connected with the route of immunization and the induction of mucosal immunity.

Determining NV CoPs will facilitate phase 3 NV vaccine field trials by substituting disease or infection end points (*23*). NV field efficacy studies are prohibitively challenging because of the short time frame and unpredictability of NV outbreaks (*48*). This was recently illustrated in a report of the first-in-human field efficacy study for an NV vaccine candidate (*12*). More than 4500 US Navy recruits were enrolled to receive the TAK-214 intramuscular vaccine targeting GI.1 and GII.4 NV and were monitored for 45 days. In year one, only eight cases occurred, no NV outbreaks were recorded, and the study was extended for a second year. In year two, 40 additional infected participants were included. In total, only eight homotypic NV cases were detected, and the primary end point was not evaluable. Despite this, efficacy was demonstrated against heterotypic NV, indicating cross-genotype protection (*12*). The data from our study indicate that fecal IgA abundance and serum NBAA titers together can estimate vaccine-induced protection against NV exposure.

There are several limitations with this study. First, controlled challenge studies routinely use an infectious dose that is three to five orders of magnitude more than typically seen with natural exposure to increase attack rates, and in this study, most individuals reported symptoms, most likely because of the high challenge inoculum. Although this approach ensures that a sufficient proportion of participants becomes infected for efficacy analyses, the large infectious dose may hinder the immune system's ability to control the infection, potentially leading to an underestimation of vaccine efficacy in challenge studies compared with field trials. As an example, in the 2016–2017 influenza challenge study by Liebowitz *et al.* (*22*), the efficacy of the approved Fluzone vaccine in the challenge was 27%, yet the reported efficacy against H1 influenza in field surveillance during the 2016–2017 flu season was 40% (*49*). This discrepancy in viral inoculum highlights how challenge models may not fully capture the protective potential of vaccines under natural exposure conditions. Second, the placebo group attack rate for NV infection was higher than anticipated in our study (82%), but the NV gastroenteritis attack rate (54%) was comparatively much lower, potentially reducing the power to detect a statistically significant difference in disease outcomes. This could have been one reason why we did not observe statistical differences between AGE or modified Vesikari scores

between the placebo and VXA-G1.1-NN groups. One additional explanation is that NV infection has a rapid onset and is characterized by acute severe symptoms that resolve quickly, providing a short window for reported symptoms. Moreover, it is unclear whether intestinal symptoms in this challenge study were triggered by active NV replication or by the large inoculum. Despite these limitations, we observed reduced presentation of emesis in the VXA-G1.1-NN–vaccinated participants. Last, this study specifically investigated NV GI.1; however, the genotype GII.4 has been more prevalent in the past 20 years (*40*). The GII.4 challenge model has not been available for several years but is expected to be reestablished (NCT04174560). To this end, we have developed a bivalent vaccine that is immunogenic in a phase 2 trial (NCT05626803), and this vaccine is currently being evaluated for the production of IgA in breast milk in nursing mothers in South Africa (South African National Clinical Trials Register: DOH-27-072023-7893).

In summary, the results of this study highlight the distinctive immunological profile of oral vaccination with VXA-G1.1-NN and demonstrate its effectiveness in protecting against NV infection and reducing shedding in stool and emesis. VXA-G1.1-NN has the potential to block mucosal transmission in semiclosed environments such as schools, nursing homes, hospitals, military bases, and child care centers, where NV spreads rapidly from person to person. VXA-G1.1-NN is formulated as a thermostable tablet, thus reducing the need for specialized infrastructure or skilled practitioners to administer the vaccine, facilitating rapid distribution. Our machine learning analyses revealed critical immune CoPs enabling focused efforts to optimize and progress promising vaccine candidates. The CoPs identified in this study will serve as critical benchmarks for evaluating future NV vaccine clinical candidates. A second-generation oral bivalent NV candidate is already in clinical development (NCT05626803) and is anticipated to further enhance protective efficacy.

MATERIALS AND METHODS

Study design

This was a phase 2b randomized, double-blind, placebo-controlled vaccination and challenge study to assess the protective efficacy of the VXA-G1.1-NN vaccine. To accommodate the limited size of the isolation unit used for the challenge and postchallenge isolation period, participants transitioned through the study (enrollment, vaccination spanning D1 to D28, and challenge spanning C1 to C8) sequentially in a total of 16 cohorts. Participants were randomized in a 1:1 ratio to receive one oral dose of vaccine or placebo in cohorts of ~5 to 12 individuals. Approximately 28 days (+30-day window) postvaccination, all participants were screened for eligibility for challenge, and each cohort was admitted to the isolation ward and challenged with the NV GI.1 Norwalk challenge strain.

A total of 523 individuals were screened against a set of inclusion and exclusion criteria. Participants with any major medical condition, laboratory finding, or electrocardiogram finding were excluded. Of these, 358 volunteers were determined to be ineligible: 217 individuals were unable or unwilling to comply with the study protocol or provide informed consent, 46 had medical issues (not healthy as deemed by the principal investigator and had major medical issues or confirmed chronic viral infections, history of cancer, gastrointestinal issues, or other conditions), and 47 had abnormal laboratory results (outside of the normal range for platelet counts or coagulation tests and abnormal electrocardiogram results). Healthy male and female adults aged 18 to 49 years (inclusive) with a body mass index of 17 to 35 kg/m^2 (inclusive) were eligible if they had blood type O or A and were confirmed H type 1 antigen secretory positive. Individuals lacking H type 1 antigen expression (secretor-negative, nonfunctional *FUT2*) exhibit resistance to GI.1 NV infection. To ensure susceptibility and consistency in study outcomes, inclusion criteria were restricted to secretor-positive individuals (H+ antigen) tested in saliva. Females were required to have a negative pregnancy test before vaccination and challenge and be at least 1 year postmenopausal or surgically sterile, use an acceptable form of contraception, or not be sexually active. Males were required to use a contraceptive barrier or remain abstinent during the active vaccination and challenge periods. Medical diagnoses or medications that could affect vaccine response, tolerability, efficacy, or AE assessments were restricted. Social or occupational circumstances that would confer risk for others were also excluded.

To calculate sample size, a two-sided Fisher's exact test (5% significance) estimated 87.2% power to detect a difference between the placebo attack rate of 40% and a VXA-G1.1-NN group attack rate of 12% when the sample size in each group was 50. Initially, 120 participants were planned for randomization and vaccination to ensure that at least 100 participants were available to participate in the viral challenge. An interim analysis reassessed the assumptions used for the primary efficacy end point after ~50 randomized participants were vaccinated and completed the challenge. Because the first 19 participants enrolled in the trial were vaccinated with a different vaccine lot than subsequent participants, an additional 20 participants were enrolled. Furthermore, a new sublot of the virus inoculum was needed to complete the challenge of these additional participants, so an additional 30 participants were enrolled. In total, ~170 participants were randomized and vaccinated to ensure that at least 140 participants were available to participate in the viral challenge.

The viral challenge was provided in distilled water as a single oral dose of NV GI.1 (Norwalk virus inoculum lot 001-09NV and sublot 2, IND 14697) at a dose of 1×10^6 genomic copies. This dose was expected to induce an infection in 50 to 65% of healthy adults (*50*). After challenge, participants were monitored for signs and symptoms of NV infection and AGE from C1 to discharge. Stool and emesis were collected, and excretion of NV (shedding) was monitored. NV infection was defined as the qPCR evidence of NV, detected in one or more postchallenge stool or emesis samples in 7 days postchallenge. The degree of illness was assessed using a modified Vesikari scale (*33*). Four days postchallenge (C5), participants were evaluated for signs and symptoms of AGE. If no clinical illness was present, asymptomatic participants were discharged from the isolation ward and followed with a series of outpatient visits and telephone calls. Symptomatic participants remained in the unit up to C8, at the discretion of the investigator. Participants who were discharged from the challenge unit returned on C8 to provide an additional fecal sample. Mucosal samples, sera, and PBMCs for immunogenicity testing were collected throughout the vaccination and challenge phases. AEs were recorded at each study visit.

Written informed consent was obtained from study participants before any study procedures. An independent safety monitoring committee oversaw the safety of the study at predefined intervals during the challenge period and as needed during the vaccination and challenge periods. This study was conducted in full conformity with the principles set forth in the Belmont Report: Ethical Principles and Guidelines for the Protection of Human Subjects of Research of the

US National Commission for the Protection of Human Subjects of Biomedical and Behavioral Research (18 April 1979) and codified in 45 Code of Regulations Part 46 and/or the International Council for Harmonisation (ICH) E6; 62 Federal Regulations 25691 (1997). The CONSORT (Consolidated Standards of Reporting Trials) guidelines were used to prepare this manuscript. The study protocol is registered at clinicaltrials.gov (NCT05212168) and was approved by the WCG (Western IRB Copernicus Group) Institutional Review Board.

Study objectives and measures

The primary objective of the study was to determine the efficacy of VXA-G1.1-NN against NV infection and gastroenteritis after GI.1 NV challenge. Secondary objectives were to assess the safety and tolerability of VXA-G1.1-NN. In addition, the ability of VXA-G1.1-NN to modify disease severity, the quantity and duration of NV shedding, and a set of immunogenicity parameters were quantified. The primary efficacy end point was the proportion of participants showing evidence of NV gastroenteritis, a composite end point was defined as meeting one or more definitions for AGE, and a positive NV infection was assessed by qPCR (Fig. 2A). AGE was defined as meeting any one of three categories: (i) diarrhea, categorized as ≥3 loose or liquid stools produced in any 24-hour period or >400 g of loose or liquid stools produced in any 24-hour period; (ii) vomiting, categorized as ≥2 vomiting episodes in any 24-hour period; and (iii) combined symptoms, namely, one vomiting episode and any loose or liquid stool in any 24-hour period or one vomiting episode and ≥2 constitutional symptoms (abdominal cramps or pain, nausea, bloating, loose feces, fever >37.6°C, and myalgia) in any 24-hour period. Stool was graded on a scale of 1 to 5 on the basis of consistency and water content. Exploratory efficacy end points included the proportion of participants (i) reporting AGE (fig. S2A); (ii) who were $qPCR^{-}AGE^{-}$ (Fig. 3A); (iii) who were $qPCR^{+}AGE^{-}$ (Fig. 3E); (iv) who seroconverted postchallenge (D28 to C29), defined as a greater than fourfold increase in GI.1-specific VP1 serum IgG antibody (fig. S2D); (v) who developed gastroenteritis with severity determined by the modified Vesikari score (fig. S2B); (vi) who had presentation of emesis (Fig. 3A); (vii) who had viral shedding in stool samples (Fig. 3C); and (viii) who had viral shedding in emesis samples (Fig. 3B) during the challenge phase.

Primary immunogenicity end points were (i) VP1-specific serum IgG, (ii) VP1-specific serum IgA, and (iii) HBGA blocking antibodies (by NBAA) on D28, as well as (iv) VP1-specific IgA antibody–secreting cells at D8 postvaccination (Fig. 2A). Exploratory immunogenicity end points were VP1-specific (i) fecal, (ii) saliva, and (iii) NLF IgA at D28 and C29 (Fig. 4D), as well as (iv) immunophenotyping analyses of plasmablasts (Fig. 4H and fig. S4E), compared in VXA-G1.1-NN versus placebo recipients. Further exploratory analyses investigated correlations between immunogenicity parameters and clinical efficacy. These are (i) univariable correlations (fig. S5) and (ii) multivariable analysis of the NV infection end point (Fig. 5).

Vaccine

VXA-G1.1-NN is an oral E1/E3–deleted replication-defective recombinant adenovirus serotype 5 with a double-stranded ribonucleic acid adjuvant. The vaccine vector encodes a full-length VP1 gene from NV genogroup GI.1 and adjuvant composed of a short hairpin RNA. The production of VXA-G1.1-NN was described previously (*21*). The final drug product was formulated into enteric-coated tablets administered to provide a multitablet single-administration dose of 1×10^{11} IU ± 0.5 log. The placebo control consisted of oral tablets similar in appearance and number to the active vaccine tablets.

Norovirus qPCR

Twenty percent stool suspensions were made using phosphate-buffered saline in a polypropylene tube. Undiluted samples of emesis were used for viral detection. All samples were mixed on a vortex shaker for 15 to 20 min at room temperature. Suspensions were then centrifuged at room temperature for 5 min at 12,000 rpm to pellet solid material. RNA extractions were performed using 140 μl of stool or emesis sample and 10 μl of MS2 (as internal extraction control) in the QIAamp Viral RNA mini kit on the QIAcube Connect instrument (QIAGEN) according to the manufacturer's instructions. qPCR was performed on the Applied Biosystems 7500 PCR instrument with sequence detection software version 1.5.1 using the AgPATH ID One-Step RT-PCR kit with a detection enhancer (Thermo Fisher Scientific). Primers and probes for NV GI and MS2 were chosen on the basis of previous references (*51*, *52*) and are listed in table S5. A standard curve was generated by 10-fold serial dilutions from 6×10^{6} to 6×10^{1} copies. The calculated limit of detection of 256 copies corresponded to a cycle threshold (Ct) of 37; therefore, samples with Ct values higher than 37 were considered negative. NATtrol NV GI.1 positive control, NATtrol NV negative control (ZeptoMetrix), and no template negative controls were run on each plate, and a mock extraction control containing MS2 was run with each batch of extracted samples. Cycling conditions were 45°C for 10 min, 95°C for 10 min, and then 45 cycles of 95°C for 15 s and 60°C for 1 min. The assay was qualified for use in the Laboratory for Specialized Clinical Studies at Cincinnati Children's Hospital Medical Center. Samples with MS2 Ct >35 or undetectable were diluted at 1:10 and 1:100 and retested. If MS2 was still not valid, samples were re-extracted and, if unsuccessful again, were reported as indeterminate. Ct values and NV copies per gram of stool or copies per gram of emesis were reported for each sample.

NV–blocking antibody assay

NBAA measures the ability of an antibody to block NV VLP interactions with the HBGA receptor. The assay was qualified and performed by PPD Inc. using the method described by Reeck *et al.* (*25*). Biotinylated Le^{b} HBGA was used to coat NeutrAvidin-coated plates at 2.5 μg/ml (Thermo Fisher Scientific). GI.1 VLP derived from the human embryonic kidney 293 cell line (AscentGene Inc.) was incubated in serum at 37°C for 1 hour. The mixture of GI.1 VLP and prediluted serum samples was added to Le^{b}-coated plates and incubated at 4°C for 2 hours. After washing, rabbit anti-GI.1 VLP polyclonal antisera at 1:10,000 (Thermo Fisher Scientific) were added, and samples were incubated at 4°C for 1 hour. The plates were washed, goat anti-rabbit IgG (H plus L) conjugated to horseradish peroxidase at 1:5000 (Bethyl Laboratories) was added, and samples were incubated at 4°C for 60 min. Plates were washed, and 100 μl of trimethylboron was added to all of the wells for 10 min. The reaction was stopped with the addition of 25 μl of sulfuric acid (1 M) to all wells. Plates were immediately read at an optical density of 450 nm (OD_{450}). The NBAA titer was determined to be the last dilution at which the experimental sample OD value was less than 50% of the OD value of VLP-only controls. The lower limit of quantification of serum NBAA titer was 1:25, and any results with less than the lower limit of quantification are reported as one-half of the limit of detection.

Statistical analysis

A two-sample, two-sided proportion test was used to evaluate primary efficacy end points, and two-sided *t* tests were used to evaluate D28 serum IgA, serum IgG, NBAA, and D8 ASC immunogenicity end points. Antibody parameters were $\log_{10}$ transformed to account for the skewed distribution. All tests were conducted at a significance level of $\alpha = 0.05$, and 95% CIs were calculated accordingly. The totality of evidence was assessed using a statistical method that combined these six prespecified outcomes. Test statistics for each primary end point were calculated (*z* score for the proportion test and *t* statistic for *t* tests), and the mean test statistic value was calculated. Thereafter, group assignment was permuted, and the mean test statistic was recalculated for each of the 10,000 iterations, generating a distribution of scores representing the null hypothesis that there is no vaccine effect. The number of generated mean test statistics plus one that was greater than or equal to the observed mean *z* score divided by 10,001 was the *P* value (one-sided) for assessing the totality of evidence effect. A two-sided Fisher's exact test was used to evaluate exploratory efficacy end points of proportions in GraphPad Prism 10 software. Viral shedding in emesis and stool samples and modified Vesikari scores were evaluated with a two-sided Wilcoxon signed-rank test in GraphPad Prism 10.

Dynamics of each immunogenicity end point was evaluated with a linear-mixed-effects regression model in GraphPad Prism 10 software. All tests were conducted at a significance level of $\alpha = 0.05$, and 95% CIs were calculated accordingly. Antibody parameters were $\log_{10}$ transformed to account for the skewed distribution. In addition, a pseudocount was added to ASCs for each sample, followed by $\log_{10}$ transformation. All other parameters were not transformed. For each end point, the model formula was end point ~ day + study_group + day:study_group + (1|participantID). "Day" is a categorical variable of the day postvaccination, and the study group is a categorical variable of VXA-G1.1-NN or placebo. We report two contrasts from each model, vaccination effects and differential effects. Vaccination effects examined whether end points were different between time points within each cohort (for example, $D28_{G1} - D1_{G1}$). Differential effects examined whether end points were different between study groups at each time point (for example, $D28_{G1} - D28_{G2}$). Tukey's test was applied to account for multiple comparisons. Pairwise Spearman correlations between immunogenicity parameters in the VXA-G1.1-NN study group were calculated with $\log_{10}$–fold change values (D28/D1) (figs. S3 and S4F) and with nominal values on D28 (fig. S5).

We conducted multivariable data analysis in the VXA-G1.1-NN and placebo study groups. Before modeling, antibody parameters (SerumIgG_D28, SerumIgA_D28, NasalIgA_D28, SalivaIgA_D28, NBAA_D28, and FecalIgA_D28) were $\log_{10}$ transformed. In addition, a pseudocount was added to the parameter ASC_D8 for each sample, followed by $\log_{10}$ transformation. B cell immunophenotyping parameters were not transformed. In total, 13 immune parameters were analyzed with Lasso (*38*) and random forest (*39*) models to predict NV infection classes (infected, class = 1, or not infected, class = 0). We used a repeated train-test resampling approach in all modeling to prevent overfitting and to obtain an unbiased estimate of model performance on unseen samples. At each iteration, 64% of the data were randomly assigned for model training, and the remaining 36% were assigned as a test set used to evaluate the models. Stratified resampling was used to ensure proportional resampling of class labels in training and test sets. When training both Lasso and random forest, data of the training set were scaled by subtracting the mean from each sample and then dividing by the standard deviation. Data of the test set were also scaled using the mean and standard deviation parameters of the training set. A weighted loss was used during training of Lasso and random forest to address the class imbalance present in the data. Estimation of L1 regularization for Lasso was calculated with 10 times–repeated, fivefold cross-validation within the training set. Random forest was fit with the number of trees set to 1000 and default settings for other hyperparameters. Overall, this procedure was performed for 100 iterations using different training and test sets in each iteration. Final predictions for each sample were calculated as the median test set prediction score across iterations. For Lasso and random forest models, variable importance was calculated as the median importance score across iterations. The importance score for a variable of the Lasso model was defined as the absolute value of the model coefficient. The importance score of a variable of the random forest model was determined with the decrease in node impurity (*53*). Model performance was assessed using a Wilcoxon test comparing prediction scores of NV infection classes, and model accuracy was calculated as the AUC. Data analyses were conducted in R 4.3.3 with software packages Tidymodels 1.2.0 (*54*), glmnet 4.1.8 (*55*), and ranger 0.16.0 (*53*). Where sample sizes were less than $n = 20$ per group, we have included individual level data in a supplementary spreadsheet (data file S1).

Supplementary Materials

The PDF file includes:

Materials and Methods
Figs. S1 to S6
Tables S1 to S6
Legend for data file S1

Other Supplementary Material for this manuscript includes the following:

Data file S1
MDAR Reproducibility Checklist

REFERENCES AND NOTES

1. S. M. Ahmed, A. J. Hall, A. E. Robinson, L. Verhoef, P. Premkumar, U. D. Parashar, M. Koopmans, B. A. Lopman, Global prevalence of norovirus in cases of gastroenteritis: A systematic review and meta-analysis. *Lancet Infect. Dis.* **14**, 725–730 (2014).
2. R. I. Glass, U. D. Parashar, M. K. Estes, Norovirus gastroenteritis. *N. Engl. J. Med.* **361**, 1776–1785 (2009).
3. US Centers of Disease Control, "Updated norovirus outbreak management and disease prevention guidelines," *MMWR Recomm. Rep.* **60** (no. RR-3) (2011).
4. M. Tan, Y. Tian, D. Zhang, Q. Wang, Z. Gao, Aerosol transmission of norovirus. *Viruses* **16**, 151 (2024).
5. N. Balachandran, C. P. Mattison, L. E. Calderwood, R. M. Burke, M. A. Schmidt, J. Donald, S. A. Mirza, Household transmission of viral acute gastroenteritis among participants within an integrated health care delivery system, 2014–2016. *Open Forum Infect. Dis.* **10**, ofad619 (2023).
6. R. L. Atmar, A. R. Opekun, M. A. Gilger, M. K. Estes, S. E. Crawford, F. H. Neill, D. Y. Graham, Norwalk virus shedding after experimental human infection. *Emerg. Infect. Dis.* **14**, 1553–1557 (2008).
7. S. Ramani, F. H. Neill, A. R. Opekun, M. A. Gilger, D. Y. Graham, M. K. Estes, R. L. Atmar, Mucosal and cellular immune responses to Norwalk virus. *J. Infect. Dis.* **212**, 397–405 (2015).
8. J. E. Matthews, B. W. Dickey, R. D. Miller, J. R. Felzer, B. P. Dawson, A. S. Lee, J. J. Rocks, J. Kiel, J. S. Montes, C. L. Moe, J. N. Eisenberg, J. S. Leon, The epidemiology of published norovirus outbreaks: A review of risk factors associated with attack rate and genogroup. *Epidemiol. Infect.* **140**, 1161–1172 (2012).
9. M. S. Riddle, R. I. Walker, Status of vaccine research and development for norovirus. *Vaccine* **34**, 2895–2899 (2016).
10. R. L. Atmar, F. Baehner, J. P. Cramer, E. Song, A. Borkowski, P. M. Mendelman, NOR-201 Study Group, Rapid responses to 2 virus-like particle norovirus vaccine candidate

formulations in healthy adults: A randomized controlled trial. *J. Infect. Dis.* **214**, 845–853 (2016).
11. G. Leroux-Roels, J. P. Cramer, P. M. Mendelman, J. Sherwood, R. Clemens, A. Aerssens, I. De Coster, A. Borkowski, F. Baehner, P. Van Damme, Safety and immunogenicity of different formulations of norovirus vaccine candidate in healthy adults: A randomized, controlled, double-blind clinical trial. *J. Infect. Dis.* **217**, 597–607 (2018).
12. J. Sherwood, P. M. Mendelman, E. Lloyd, M. Liu, J. Boslego, A. Borkowski, A. Jackson, D. Faix, US Navy Study Team, Efficacy of an intramuscular bivalent norovirus GI.1/GII.4 virus-like particle vaccine candidate in healthy US adults. *Vaccine* **38**, 6442–6449 (2020).
13. J. J. Treanor, R. L. Atmar, S. E. Frey, R. Gormley, W. H. Chen, J. Ferreira, R. Goodwin, A. Borkowski, R. Clemens, P. M. Mendelman, A novel intramuscular bivalent norovirus virus-like particle vaccine candidate—reactogenicity, safety, and immunogenicity in a phase 1 trial in healthy adults. *J. Infect. Dis.* **210**, 1763–1771 (2014).
14. J. Treanor, J. Sherwood, J. P. Cramer, N. Le Cam Bouveret, S. Lin, F. Baehner, A. Borkowski, NOR-204 Investigators, A phase 2 study of the bivalent VLP norovirus vaccine candidate in older adults; impact of MPL adjuvant or a second dose. *Vaccine* **38**, 5842–5850 (2020).
15. T. Vesikari, X. Saez-Llorens, V. Blazevic, P. Lopez, E. Lopez, T. Masuda, P. M. Mendelman, M. Liu, J. Sherwood, F. Baehner, A. Borkowski, Immunogenicity of a bivalent virus-like particle norovirus vaccine in children from 1 to 8 years of age: A phase 2 randomized, double-blind study. *Vaccine* **40**, 3588–3596 (2022).
16. R. L. Atmar, D. I. Bernstein, C. D. Harro, M. S. Al-Ibrahim, W. H. Chen, J. Ferreira, M. K. Estes, D. Y. Graham, A. R. Opekun, C. Richardson, P. M. Mendelman, Norovirus vaccine against experimental human Norwalk virus illness. *N. Engl. J. Med.* **365**, 2178–2187 (2011).
17. D. I. Bernstein, R. L. Atmar, G. M. Lyon, J. J. Treanor, W. H. Chen, X. Jiang, J. Vinje, N. Gregoricus, R. W. Frenck Jr., C. L. Moe, M. S. Al-Ibrahim, J. Barrett, J. Ferreira, M. K. Estes, D. Y. Graham, R. Goodwin, A. Borkowski, R. Clemens, P. M. Mendelman, Norovirus vaccine against experimental human GII.4 virus illness: A challenge study in healthy adults. *J. Infect. Dis.* **211**, 870–878 (2015).
18. S. S. El-Kamary, M. F. Pasetti, P. M. Mendelman, S. E. Frey, D. I. Bernstein, J. J. Treanor, J. Ferreira, W. H. Chen, R. Sublett, C. Richardson, R. F. Bargatze, M. B. Sztein, C. O. Tacket, Adjuvanted intranasal Norwalk virus-like particle vaccine elicits antibodies and antibody-secreting cells that express homing receptors for mucosal and peripheral lymphoid tissues. *J. Infect. Dis.* **202**, 1649–1658 (2010).
19. Y. Gao, Y. Guo, Research progress in the development of natural-product-based mucosal vaccine adjuvants. *Front. Immunol.* **14**, 1152855 (2023).
20. B. A. Flitter, S. N. Greco, C. A. Lester, E. D. Neuhaus, S. N. Tedjakusuma, M. Shriver, E. Cuevas-Juárez, S. Gutierrez, M. R. Braun, M. F. Pasetti, S. N. Tucker, J. F. Cummings, An oral norovirus vaccine tablet was safe and elicited mucosal immunity in older adults in a phase 1b clinical trial. *Sci. Transl. Med.* **17**, eads0556 (2025).
21. L. Kim, D. Liebowitz, K. Lin, K. Kasparek, M. F. Pasetti, S. J. Garg, K. Gottlieb, G. Trager, S. N. Tucker, Safety and immunogenicity of an oral tablet norovirus vaccine, a phase I randomized, placebo-controlled trial. *JCI Insight* **3**, 121077 (2018).
22. D. Liebowitz, K. Gottlieb, N. S. Kolhatkar, S. J. Garg, J. M. Asher, J. Nazareno, K. Kim, D. R. McIlwain, S. N. Tucker, Efficacy, immunogenicity, and safety of an oral influenza vaccine: A placebo-controlled and active-controlled phase 2 human challenge study. *Lancet Infect. Dis.* **20**, 435–444 (2020).
23. S. Ramani, M. K. Estes, R. L. Atmar, Correlates of protection against norovirus infection and disease—Where are we now, where do we go? *PLOS Pathog.* **12**, e1005334 (2016).
24. R. Czakó, R. L. Atmar, A. R. Opekun, M. A. Gilger, D. Y. Graham, M. K. Estes, Serum hemagglutination inhibition activity correlates with protection from gastroenteritis in persons infected with Norwalk virus. *Clin. Vaccine Immunol.* **19**, 284–287 (2012).
25. A. Reeck, O. Kavanagh, M. K. Estes, A. R. Opekun, M. A. Gilger, D. Y. Graham, R. L. Atmar, Serological correlate of protection against norovirus-induced gastroenteritis. *J. Infect. Dis.* **202**, 1212–1218 (2010).
26. R. L. Atmar, D. I. Bernstein, G. M. Lyon, J. J. Treanor, M. S. Al-Ibrahim, D. Y. Graham, J. Vinjé, X. Jiang, N. Gregoricus, R. W. Frenck, C. L. Moe, W. H. Chen, J. Ferreira, J. Barrett, A. R. Opekun, M. K. Estes, A. Borkowski, F. Baehner, R. Goodwin, A. Edmonds, P. M. Mendelman, Serological correlates of protection against a GII.4 norovirus. *Clin. Vaccine Immunol.* **22**, 923–929 (2015).
27. K. Tamminen, M. Malm, T. Vesikari, V. Blazevic, Norovirus-specific mucosal antibodies correlate to systemic antibodies and block norovirus virus-like particles binding to histo-blood group antigens. *Clin. Immunol.* **197**, 110–117 (2018).
28. R. L. Atmar, J. P. Cramer, F. Baehner, C. Han, A. Borkowski, P. M. Mendelman, An exploratory study of the salivary immunoglobulin A responses to 1 dose of a norovirus virus-like particle candidate vaccine in healthy adults. *J. Infect. Dis.* **219**, 410–414 (2019).
29. A. Dey, N. A. Molodecky, H. Verma, P. Sharma, J. S. Yang, G. Saletti, M. Ahmad, S. K. Bahl, T. F. Wierzba, R. K. Nandy, J. M. Deshpande, R. W. Sutter, C. Czerkinsky, Human circulating antibody-producing B cell as a predictive measure of mucosal immunity to poliovirus. *PLOS ONE* **11**, e0146010 (2016).
30. L. Kim, C. J. Martinez, K. A. Hodgson, G. R. Trager, J. R. Brandl, E. P. Sandefer, W. J. Doll, D. Liebowitz, S. N. Tucker, Systemic and mucosal immune responses following oral adenoviral delivery of influenza vaccine to the human intestine by radio controlled capsule. *Sci. Rep.* **6**, 37295 (2016).
31. L. J. Wei, J. M. Lachin, Two-sample asymptotically distribution-free tests for incomplete multivariate observations. *J. Am. Stat. Assoc.* **79**, 653–661 (1984).
32. D. Li, C. M. McDonald, G. L. Elfring, M. Souza, J. McIntosh, D. H. Kim, L. J. Wei, Assessment of treatment effect with multiple outcomes in 2 clinical trials of patients with Duchenne muscular dystrophy. *JAMA Netw. Open* **3**, e1921306 (2020).
33. S. B. Freedman, M. Eltorky, M. Gorelick, Pediatric Emergency Research Canada Gastroenteritis Study Group, Evaluation of a gastroenteritis severity score for use in outpatient settings. *Pediatrics* **125**, e1278–e1285 (2010).
34. D. Li, L. Baert, E. Van Coillie, M. Uyttendaele, Critical studies on binding-based RT-PCR detection of infectious Noroviruses. *J. Virol. Methods* **177**, 153–159 (2011).
35. D. Hobson, R. L. Curry, A. S. Beare, A. Ward-Gardner, The role of serum haemagglutination-inhibiting antibody in protection against challenge infection with influenza A2 and B viruses. *J. Hyg.* **70**, 767–777 (1972).
36. P. C. Johnson, J. J. Mathewson, H. L. DuPont, H. B. Greenberg, Multiple-challenge study of host susceptibility to Norwalk gastroenteritis in US adults. *J. Infect. Dis.* **161**, 18–21 (1990).
37. I. D. Plumb, L. M. Fette, A. H. Tjaden, L. Feldstein, S. Saydah, A. Ahmed, R. Link-Gelles, T. F. Wierzba, A. A. Berry, D. Friedman-Klabanoff, M. P. Larsen, M. S. Runyon, L. M. Ward, R. P. Santos, J. Ward, W. S. Weintraub, S. Edelstein, D. Uschner, Estimated COVID-19 vaccine effectiveness against seroconversion from SARS-CoV-2 infection, March-October, 2021. *Vaccine* **41**, 2596–2604 (2023).
38. R. Tibshirani, Regression shrinkage and selection via the lasso: A retrospective. *J. R. Stat. Soc. B Stat. Methodol.* **73**, 273–282 (2011).
39. L. Breiman, Random forests. *Mach. Learn.* **45**, 5–32 (2001).
40. B. A. Lopman, D. Steele, C. D. Kirkwood, U. D. Parashar, The vast and varied global burden of norovirus: Prospects for prevention and control. *PLoS Med.* **13**, e1001999 (2016).
41. P. F. Teunis, F. H. Sukhrie, H. Vennema, J. Bogerman, M. F. Beersma, M. P. Koopmans, Shedding of norovirus in symptomatic and asymptomatic infections. *Epidemiol. Infect.* **143**, 1710–1717 (2015).
42. P. J. Marks, I. B. Vipond, D. Carlisle, D. Deakin, R. E. Fey, E. O. Caul, Evidence for airborne transmission of Norwalk-like virus (NLV) in a hotel restaurant. *Epidemiol. Infect.* **124**, 481–487 (2000).
43. P. J. Marks, I. B. Vipond, F. M. Regan, K. Wedgwood, R. E. Fey, E. O. Caul, A school outbreak of Norwalk-like virus: Evidence for airborne transmission. *Epidemiol. Infect.* **131**, 727–736 (2003).
44. M. R. Evans, R. Meldrum, W. Lane, D. Gardner, C. D. Ribeiro, C. I. Gallimore, D. Westmoreland, An outbreak of viral gastroenteritis following environmental contamination at a concert hall. *Epidemiol. Infect.* **129**, 355–360 (2002).
45. D. F. King, H. Groves, C. Weller, I. Jones, J. P. Cramer, P. B. Gilbert, D. Goldblatt, M. F. Gruber, B. Kampmann, D. Maïga, M. F. Pasetti, S. A. Plotkin, A. Precioso, L. Wassie, F. Wittke, D. C. Kaslow, Realising the potential of correlates of protection for vaccine development, licensure and use: Short summary. *NPJ Vaccines* **9**, 82 (2024).
46. M. Malm, H. Uusi-Kerttula, T. Vesikari, V. Blazevic, High serum levels of norovirus genotype-specific blocking antibodies correlate with protection from infection in children. *J. Infect. Dis.* **210**, 1755–1762 (2014).
47. P. López, E. López-Medina, X. Sáez-Llorens, R. deAntonio, T. Masuda, P. M. Mendelman, J. Sherwood, F. Baehner, A. Borkowski, Immunogenicity and tolerability of a bivalent virus-like particle norovirus vaccine candidate in children from 6 months up to 4 years of age: A phase 2 randomized, double-blind trial. *Hum. Vaccin. Immunother.* **19**, 2204787 (2023).
48. J. P. Harris, B. A. Lopman, S. J. O'Brien, Infection control measures for norovirus: A systematic review of outbreaks in semi-enclosed settings. *J. Hosp. Infect.* **74**, 1–9 (2010).
49. B. Flannery, J. R. Chung, A. S. Monto, E. T. Martin, E. A. Belongia, H. Q. McLean, M. Gaglani, K. Murthy, R. K. Zimmerman, M. P. Nowalk, M. L. Jackson, L. A. Jackson, M. A. Rolfes, S. Spencer, A. M. Fry, US Flu VE Investigators, Influenza vaccine effectiveness in the United States during the 2016–2017 season. *Clin. Infect. Dis.* **68**, 1798–1806 (2019).
50. R. Mateo, L. C. Lindesmith, S. J. Garg, K. Gottlieb, K. Lin, S. Said, J. S. Leon, A. C. Sims, D. J. Weber, R. S. Baric, S. N. Tucker, D. N. Taylor, Production and clinical evaluation of Norwalk GI.1 virus lot 001-09NV in norovirus vaccine development. *J. Infect. Dis.* **221**, 919–926 (2020).
51. A. A. Trujillo, K. A. McCaustland, D. P. Zheng, L. A. Hadley, G. Vaughn, S. M. Adams, T. Ando, R. I. Glass, S. S. Monroe, Use of TaqMan real-time reverse transcription-PCR for rapid detection, quantification, and typing of norovirus. *J. Clin. Microbiol.* **44**, 1405–1412 (2006).
52. J. L. Cannon, L. Barclay, N. R. Collins, M. E. Wikswo, C. J. Castro, L. C. Magaña, N. Gregoricus, R. L. Marine, P. Chhabra, J. Vinjé, Genetic and epidemiologic trends of norovirus outbreaks in the United States from 2013 to 2016 demonstrated emergence of novel GII.4 recombinant viruses. *J. Clin. Microbiol.* **55**, 2208–2221 (2017).

53. M. N. Wright, A. Ziegler, Ranger: A fast implementation of random forests for high dimensional data in C++ and R. *J. Stat. Softw.* **77**, 1–17 (2017).
54. M. Kuhn, H. Wickham, "Tidymodels: A collection of packages for modeling and machine learning using tidyverse principles" (2020); https://cran.r-project.org/web/packages/tidymodels/citation.html; www.tidymodels.org/.
55. J. Friedman, T. Hastie, R. Tibshirani, Regularization paths for generalized linear models via coordinate descent. *J. Stat. Softw.* **33**, 1–22 (2010).

Acknowledgments: We would like to acknowledge the editorial assistance of R. Perry and J. Newman in the preparation of this manuscript, which was supported by Vaxart Inc. The authors would like to acknowledge PPD Inc., in particular C. Breidenbach and O. Briskin, for efforts with assay qualification and serum VP1-specific IgG and IgA Meso Scale Discovery immunoassay and NBAA testing. **Funding:** This study was funded by Vaxart Inc. **Author contributions:** J.F.C., S.N.T., S.N.G., and M.D.A. designed the study. J.F.C., M.D.A., N.P.D., S.N.G., L.Q.N., and B.A.F. supervised the clinical trial and biosample logistics. L.C.L. and R.S.B. provided the GI.1 challenge material. S.N.G. and L.Q.N. conducted medical monitoring and pharmacovigilance oversight. J.F.C., S.N.T., L.-J.W., R.W.F., M.F.P., and B.A.F. determined the methodology used for experimental analysis. B.A.F. supervised external and internal immunogenicity testing. E.D.N., D.C.M.H., and M.S. conducted ASC testing, flow cytometry, and NLF testing. M.S. conducted saliva and fecal IgA testing. C.Q. conducted emesis and stool NV qPCR experiments. J.G., S.N.G., L.-J.W., and B.A.F. conducted the formal data analysis. J.G. provided data visualization and machine learning analysis. S.N.G., B.A.F., and J.G. wrote the original draft. B.A.F., J.G., S.N.G., R.W.F., M.F.P., S.N.T., and J.F.C. reviewed and edited the manuscript. **Competing interests:** S.N.G., B.A.F., N.P.D., M.D.A., E.D.N., D.C.M.H., S.N.T., and J.F.C. are employees and shareholders of Vaxart Inc., which funded this study. J.G. is a paid consultant of Vaxart. The experiments were designed and analyzed by Vaxart Inc. using material developed by Vaxart Inc. L.Q.N. is an employee of Amgen. L.C.L. and R.S.B. have ongoing collaborations with GIVAX, Vaxart, MERK, Takeda Vaccines, and Maine Biotech that are unrelated and do not pose conflicts of interest with this report. R.S.B. is on the scientific advisory board of Invivyd Inc. R.W.F. is currently a data and safety monitoring board member for other Vaxart clinical studies and did not serve as a data and safety monitoring board member for the clinical protocol reported in this manuscript. S.N.T. is named as an inventor on the patent covering the vaccine platform: "Formulations for small intestinal delivery of rsv and norovirus antigens" (US patent numbers 11,433,146 and 12,186,407). S.N.T., L.C.L., and R.S.B. hold patents on NV vaccine design and therapeutics "Antibodies targeting GII.4 variants and GII genotypes of human norovirus" (US patent application no. 63/656,263). The other authors declare that they have no competing interests. **Data and materials availability:** All data associated with this study are in the paper or Supplementary Materials. The code to replicate analyses presented in this manuscript is available at Zenodo (https://zenodo.org/records/15178451; DOI: 10.5281/zenodo.15178451).

Submitted 27 November 2024
Accepted 17 April 2025
Published 14 May 2025
10.1126/scitranslmed.adh9906

Science Translational Medicine
AAAS

Supplementary Materials for

An oral norovirus vaccine generates mucosal immunity and reduces viral shedding in a phase 2 placebo-controlled challenge study

Becca A. Flitter *et al.*

Corresponding author: Becca A. Flitter, bflitter@vaxart.com; James F. Cummings, jcummings@vaxart.com

Sci. Transl. Med. **17**, eadh9906 (2025)
DOI: 10.1126/scitranslmed.adh9906

The PDF file includes:

Other Supplementary Material for this manuscript includes the following:

SUPPLEMENTAL MATERIALS AND METHODS

IgG and IgA serum MSD assay

MSD U-PLEX plates (Meso Scale Discovery) were used to measure serum IgG and IgA antibodies to norovirus GI.1 VLP. The assay was conducted under qualified conditions performed by PPD, Inc. The U-PLEX plates were coated with 66 nM of biotinylated GI.1 VLP (AscentGene, Inc.) according to manufacturer instructions. Serum was diluted 1:1600 and 1:16000 in 1% ECL Blocking Agent (Cytiva) in 1X phosphate buffered saline (PBS) and 0.05% Tween 20, assayed in duplicate, and incubated at room temperature for two hours shaking at 700 rpm. A qualified standard pre-screened for antibodies to norovirus was serially diluted 4-fold and included in all assays. Plates were washed with 1X PBS, 0.05% Tween 20, and incubated with a 1:200 dilution of 200X MSD Sulfo-Tag anti-IgG or IgA for 1 hour shaking at 700 rpm. Plates were washed with 1X PBS, 0.05% Tween 20 and developed using MSD gold read buffer. Data were acquired using the MSD Sector Imager 120 instrument and expressed as MSD arbitrary units (AU) /mL.

VP1 IgA antibody secreting cell (ASC) analysis

Cryopreserved peripheral blood mononuclear cells (PBMCs) isolated on day 1 (D1) and D8 were used for determining GI.1 VP1-specific IgA ASCs by ELISpot. PBMCs were thawed and washed with 1X Anti-Aggregate Solution (ImmunoSpot) in RPMI-1640 (Lonza). 96-Well Filter Plates (MabTech) were coated with anti-human IgA (MT57, MabTech) antibody and incubated at 4°C for 16 hours. Plates were washed 6 times with sterile 1X PBS and blocked with 1% L-Glutamine, penicillin and streptomycin (Sigma) CTL-Test Assay Solution (ImmunoSpot) for 2 hours at room temperature. 100 µL of PBMCs at concentrations of $3x10^5$ cells/mL and $1x10^5$ cells/mL in CTL-Test media. After a 16-hour incubation at 37°C and 5% CO2, plates were washed and biotinylated anti-IgA antibody at 1 µg/mL (MT20, MabTech) in 0.5% fetal bovine serum (FBS) was added for 2 hours. Detection streptavidin-horseradish peroxidase (HRP) (MabTech) in 0.5% FBS 1X PBS was added at room temperature for 1 hour. The plates were washed and 100µL of AEC Substrate (Vector Labs, Newark, CA, USA) was added and developed in the dark for 4 minutes at room temperature before washing with tap water for 3 minutes prior to analysis. Analysis was done using an automated ELISpot reader system (Zeiss) and spot counts were normalized to $1x10^6$ PBMCs.

B cell immunophenotyping

For B cell immunophenotyping, PBMCs isolated on days 1 and 8 were stained with 8 color antibody panel and assessed by flow cytometry (Attune Nxt, Thermo Fisher). Thawed PBMCs were washed with 10 mL thaw solution (CTL Anti-Aggregate 20X, CTL ImmunoSpot and RPMI-1640, Gibco). Cells were resuspended in 180 µL FACS buffer (1X DPBS and 5% heat inactivated FBS) for a $1x10^7$ cells/mL suspension. 1µg/µl of Fc block (BD Pharmingen) added to cell suspension and incubated at 4˚C for 20 mins. PBMCs were surface stained (see list of antigens and fluorophores in **table S6**) for 60 mins at 4˚C in the dark with a 1:100 dilution of the antibody panel in FACS buffer. Cells were washed with FACS buffer then fixed with 2% paraformaldehyde in PBS (Biotium) for 15 minutes. Stained cells were washed and resuspended in 200 µL PBS for acquisition on an Attune NxT flow cytometer. Data were analyzed with FlowJo 10.

IgA detection in nasal lining fluid by MSD

Two synthetic absorptive matrix (SAM) Nasosorption FX-i devices (Mucosal Diagnostics) were used to collect nasal lining fluid from the left and right nasal cavity on D1, D28, and challenge day 29 (C29) according to manufacturer's instructions. The right and left SAM Nasosorption FX-i devices were immediately stored at -80°C. To extract antibodies from the nasal lining fluid, SAM Nasosorption FX-i devices were thawed at room temperature, and the absorbent tips were cut and placed into Eppendorf tubes containing 300 µL elution buffer (0.05% Tween, 1% bovine serum albumin, 1X PBS). After vortexing for 30 seconds, the resulting eluent liquid and absorbent tip were transferred into pre-charged Costar Spin-X 0.22 µm centrifuge filters (Corning). The centrifuge columns were spun at 16,000 g at 4°C for 20 minutes to filter the elution. The left and right nasal eluants were then pooled and stored at -80°C. Antigen-specific nasal IgA was measured using 2-Assay U-PLEX plates. Nasal lining fluid was diluted at 1:5, 1:10, and 1:100 in 1% ECL Blocking Agent and incubated on the plates according to manufacturer's instructions. Plates were read on a Meso QuickPlex instrument, and antigen-specific IgA signals were reported in relative light units (RLU). Nasal lining fluid was diluted 1:1000 and 1:5000 in 1% ECL Blocking Agent and incubated on GOLD 96-well small spot streptavidin plates for measurement of total IgA. Plates were read on a Meso QuickPlex instrument, and sample antibody concentrations were reported in ng/mL as calculated from an IgA standard curve. Antigen-specific nasal IgA was normalized to the total amount of IgA in the corresponding sample to get final values of RLU per µg/total IgA.

GI.1 VP1-specific saliva IgA ELISA

Saliva was collected using Salivettes (Sarstedt) on D1, D28, and C29 according to manufacturer instructions. One Salivette was collected for each timepoint and aliquoted and immediately frozen and stored at -80˚C. For total saliva IgA determinations, Immulon 2HB microtiter plates (Thermo Scientific) were coated with purified goat anti-human IgA (α-chain specific) from Jackson ImmunoResearch at 1 µg/ml in PBS and incubated for 3 h at 37°C. To measure norovirus-specific antibodies, Immulon 2HB plates were coated with norovirus GI.1 VLP (AscentGene) at 1 µg/ml in PBS and incubated for 3 h at 37°C. After incubation, plates were washed with PBS containing 0.05% Tween 20 (PBST) and blocked overnight at 4˚C with PBS containing 10% nonfat dry milk (NFDM) (Nestlé, Carnation brand). Saliva samples were diluted in PBST + 10% NFDM for initial testing at 1:10,000 for total IgA or at 1:10 for norovirus-specific IgA measurements. For total IgA, Human IgA purified from plasma (Calbiochem) was serially diluted two-fold from 12.6 ng/ml in PBST + 10% NFDM to generate a seven-point standard curve. Likewise, a norovirus IgA positive in-house standard was serially diluted and included for GI.1 VLP-specific IgA measurement. Clinical samples and standards were added to plates in duplicate, and plates were incubated for 1 h at 37°C. After washing with PBST, HRP-labeled α-specific goat anti-human IgA (Jackson ImmunoResearch) was diluted in PBST + 10% NFDM at 1:10,000 for total IgA or 1:2,000 for norovirus-specific IgA detection and added to all wells. Plates were incubated for 1 h at 37°C. Following incubation and washing, TMB Microwell Peroxidase Substrate (SeraCare) was added, and plates were incubated for 15 minutes in the dark (with agitation) at ambient temperature. The colorimetric reaction was stopped by the addition of 1 M phosphoric acid to all wells. Optical density at 450 nm (OD_{450}) were read using a Multiskan FC Microplate Reader (Thermo Scientific, cat. 51119000). The mean OD_{450} values of blank wells (PBST + 10% NFDM only) were subtracted from the absorbance values (OD_{450}) of samples and standard wells (mean OD_{450} values of duplicate wells). The absorbance values of the

standards were analyzed by linear regression analysis. IgA concentrations were determined by interpolation from the standard curve. Results were reported as a ratio of norovirus-specific IgA to total IgA. The lower limit of quantification (LLOQ) for salivary IgA was 3.0 ng/ml, and any results <LLOQ were reported as 1.5 ng/ml.

Stool supernatant extraction for ELISA

Whole stool (200 mg) was transferred to a 2 ml conical tube containing 500 mg of 2.3 mm zirconia silica beads and 1 ml extraction buffer (soybean trypsin inhibitor (STI), ethylenediaminetetraacetic acid (EDTA) solution, 1X PBS pH 7.4, phenylmethanesulfonylfluoride (PMSF) solution). Stool specimens were homogenized for 1 min at 4°C and centrifuged at 14,000 x g for 30 min. The resulting supernatants were then collected, stabilization-preservative buffer (10% bovine serum albumin in PBS and 1% sodium azide in sterile water) at a 1:50 ratio was added, and supernatants stored at -80°C until they were assayed.

Fecal norovirus and total IgA ELISA

For total IgA and norovirus-specific IgA determinations, medium-binding microtiter plates (Greiner Bio-One) were coated with 1 μg/ml purified goat anti-human IgA (α-chain specific) (Jackson ImmunoResearch) or 0.5 μg/ml norovirus GI.1 VLP (AscentGene), respectively, diluted in 1X PBS. Plates were incubated overnight at 4°C. After coating incubation, plates were washed three times with PBST. Blocking buffer, PBST containing 10% NFDM (Nestlé), was added to all wells, and plates were incubated for 1 h at 37°C. Samples, standards, and assay controls were diluted in PBST with 10% NFDM. Stool supernatants were initially prepared at 1:10 and 1:10,000 dilutions for specific and total IgA, respectively. For total IgA quantification, Human IgA purified from plasma (Calbiochem) was serially diluted two-fold from 15.4 ng/ml to generate a seven-point standard. Likewise, a norovirus IgA positive in-house standard was serially diluted and included for GI.1 VLP-specific IgA measurement. Clinical samples, standards, controls, and diluent-only blanks were added to plates in duplicate, and plates were incubated for 1 h at 37°C. Then plates were washed as described above, HRP-labeled α-specific goat anti-human IgA (Jackson ImmunoResearch) was diluted in PBST + 10% NFDM at 1:50,000 for both ELISAs and added to all wells. Plates were again incubated for 1 h at 37°C. Following incubation and washing, TMB Microwell Peroxidase Substrate (SeraCare) was added, and plates were incubated for 15 minutes in the dark (with agitation) at ambient temperature. The colorimetric reaction was stopped by the addition of 1M phosphoric acid to all wells. Absorbance, optical density at 450 nm (OD_{450}), was read using a Multiskan FC Microplate Reader (Thermo Scientific). Absorbance values of duplicate wells were averaged and the mean OD_{450} of blank wells (PBST + 10% NFDM only) were subtracted. The net mean OD_{450} values of the standards were analyzed by four-parameter logistics (4PL). Total and specific IgA concentrations (μg/ml) in diluted clinical samples were interpolated from the standards by backfitting the OD_{450} values produced by samples to the corresponding standard curves. Results were reported as a ratio of norovirus-specific IgA to total IgA.

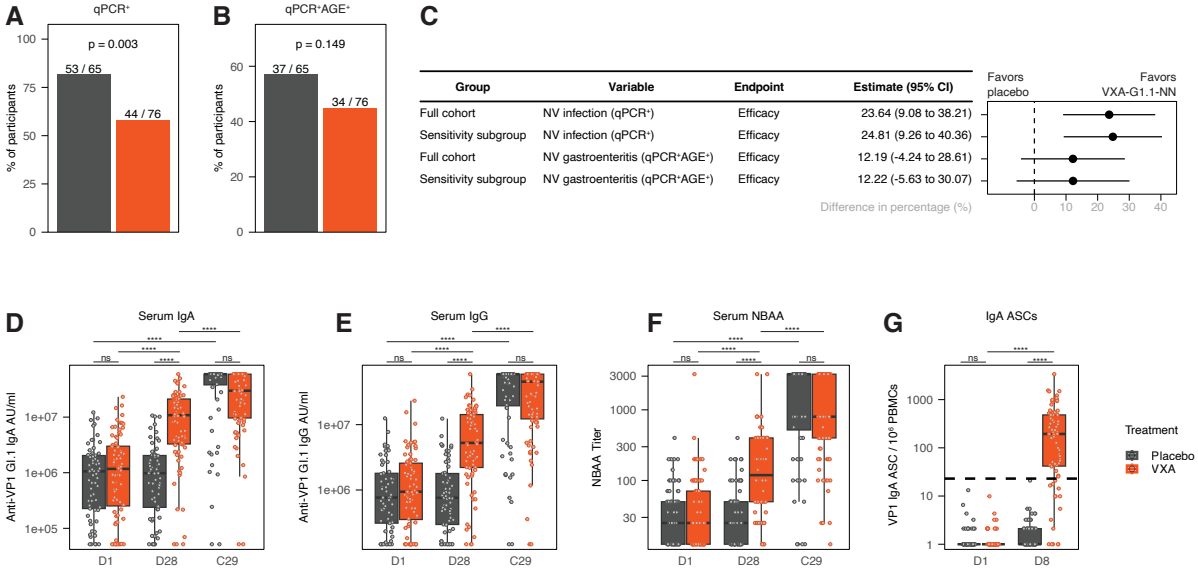

Figure S1. Primary efficacy and immunogenicity endpoints analyses. (**A and B**) The proportion of participants in VXA-G1.1-NN or placebo study groups who were qPCR$^+$ for detection of norovirus viral RNA in at least one emesis or stool sample (A), or both qPCR$^+$ and presented with acute gastroenteritis (AGE$^+$) during the challenge phase (B). Data in (A and B) are presented as ratios of positive cases among the total study group. (**C**) A sensitivity analysis excluding N = 21 (N = 9 in VXA, N = 12 placebo) participants who received the challenge further than 29 days and up to 56 days post-vaccination. Table and forest plot of results for individual primary efficacy endpoints are shown with estimates of the difference between placebo and VXA-G1.1-NN with 95% confidence intervals. Data are for the full cohort (VXA, N = 76 and placebo, N = 65); and sensitivity subgroup (VXA, N = 67 and placebo N = 53). For (A to C), differences of ratios between study groups were tested with the two-sample proportions test. (**D to F**) Serum antibody immunogenicity readouts including VP1 IgA (D) and IgG values (E), as well as serum blocking titer as measured by the norovirus blocking antibody assay (NBAA; F). AU, arbitrary units. Data in (D to F) are N = 76 for the VXA-G1.1-NN and N = 64 or 65 for the placebo study groups. (**G**) VP1 IgA ASCs were quantified by ASC assay in PBMC samples. The number of ASCs per 1x10^6 PBMCs is shown. The dashed line indicates ASC responder threshold = 23 spots per 1x10^6 PBMCs. Data for (F) are N = 65 and N = 74 for the placebo and VXA-G1.1-NN study groups, respectively. Data are shown at pre-vaccination baseline (D1), eight- or twenty-eight-days post vaccination (D8, D28) and twenty-nine days post challenge (C29). Data are presented on each study day for VXA-G1.1-NN and placebo study groups as boxplots, with bounds from 25th to 75th percentile, median line, and whiskers, which extend to the largest or smallest value no further than 1.5 * the interquartile range. Points correspond to a sample from each participant. P-values and significance in (D to G) were calculated with a linear mixed-effects model fitting each antibody measurement as the outcome and time, study group, and their interaction as main effects. Participant ID was fitted as a random effect. **p < 0.01; ***p < 0.001; ****p < 0.0001; ns, not significant.

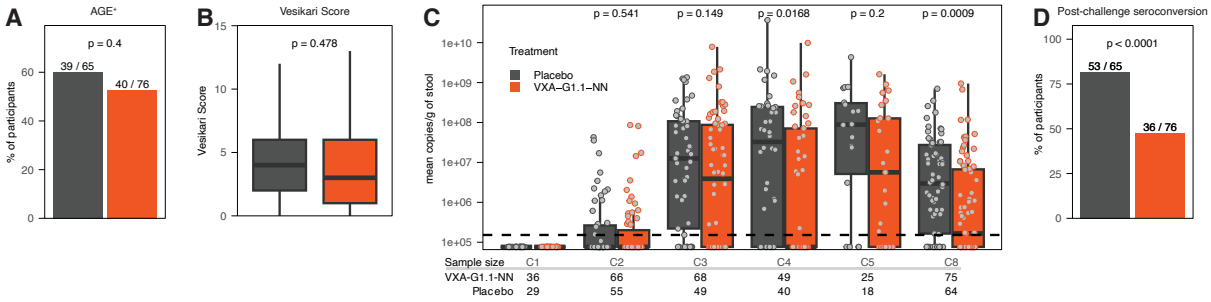

Figure S2. Exploratory efficacy endpoints analyses. (**A**) The proportion of participants in VXA-G1.1-NN or placebo study groups who presented acute gastroenteritis (AGE^{+}) during the challenge phase. (**B**) The Vesikari gastroenteritis severity score is shown for each study group. Data are N = 65 in the placebo group and N = 76 participants in the VXA-G1.1-NN study group. (**C**) Genomic copies of viral RNA per gram of stool from participants in each study group. Each data point corresponds to the geometric mean of stool samples collected for each participants on each of the indicated study days. The dashed line indicates the limit of detection. The number of participants in each study group on each study day is indicated on the bottom margin. (**D**) Participants were classified for post-challenge seroconversion if there was greater than a 4-fold increase in VP1 serum IgG antibody concentrations from D28 (pre-norovirus challenge, post-vaccination) to C29 (post-norovirus challenge). The proportion of participants who seroconverted is shown. Data in (A, and D) are presented as ratios of positive cases among the total study group, and differences of ratios between study groups were tested with two-sided Fisher's exact test. Data in (B and C) are presented as a box plots, with bounds from 25th to 75th percentile, median line, and whiskers, which extend to the largest or smallest value no further than 1.5 * the interquartile range. Statistical significance in (B and C) was calculated with a two-sided Wilcoxon test and nominal p-values are shown within the plots.

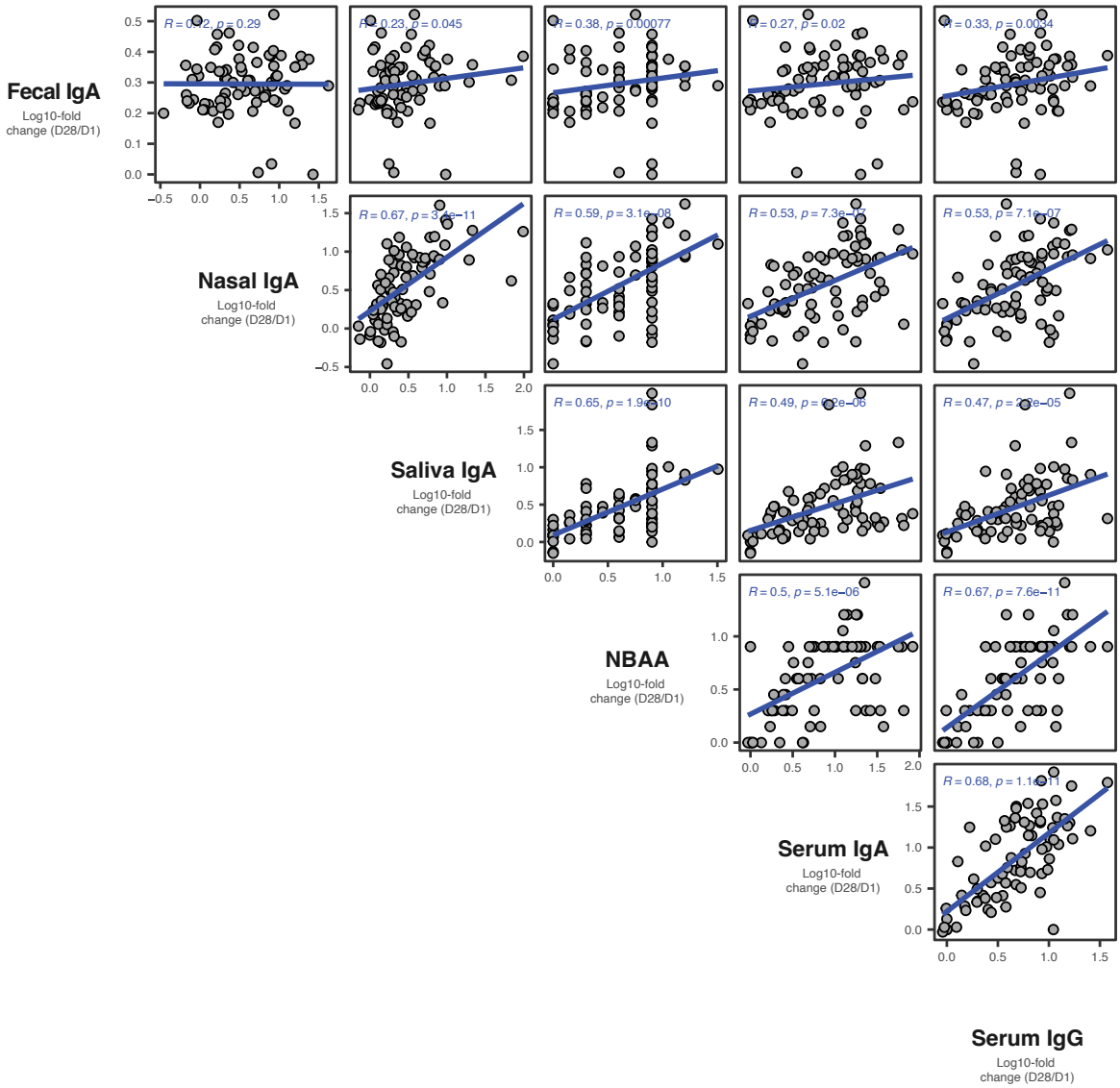

Figure S3. Serum and mucosal antibody responses stimulated by VXA-G1.1-NN are intercorrelated. Scatterplot matrix representing Spearman correlations between pairs of log10-transformed fold-changes (D28 / D1) of the following antibody parameters: serum VP1-specific IgA and IgG, saliva, nasal, and fecal VP1 IgA, and serum norovirus blocking antibody assay (NBAA). Correlation coefficients and associated p-values are shown in blue, and a regression line is depicted. Data are from N = 76 participants in the VXA-G1.1-NN study group.

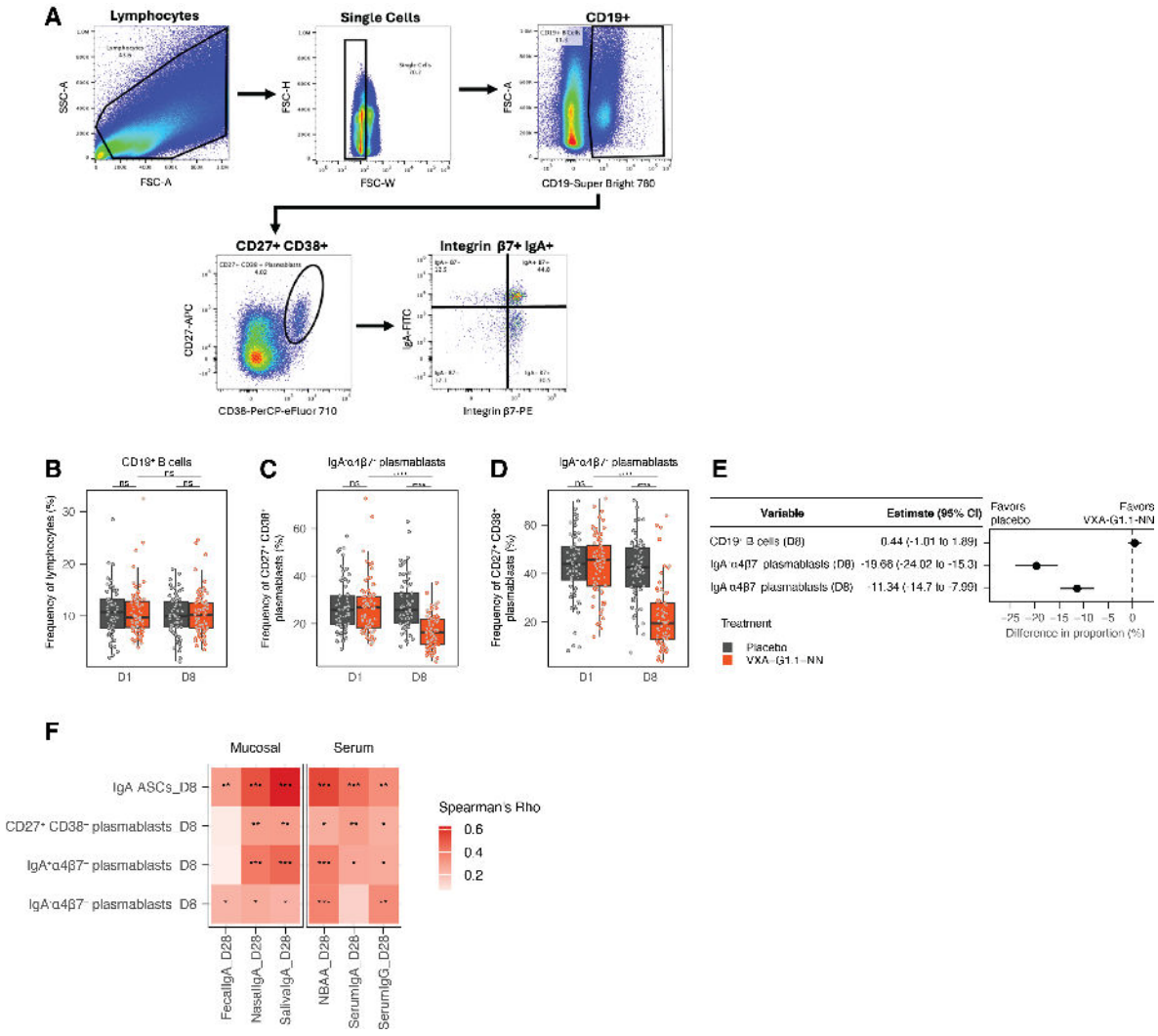

Figure S4. Mucosal-homing B cell immunophenotyping. (**A**) Flow cytometry gating strategy for the identification of plasmablasts expressing IgA and integrin α4β7 in PBMCs. B cell and plasmablasts populations were classified according to the expression of CD19, CD27, CD38, IgA, and α4β7. Bivariate dot plots are shown for the identification of $CD19^+$ B cells and $CD27^+CD38^+$ plasmablasts. $CD27^+CD38^+$ cells were further stratified by IgA^+ and $\alpha4\beta7^+$ expression. (**B to D**) Frequencies of $CD19^+$ B cells among $CD45^+$ cells (B) and of IgA^- $\alpha4\beta7^-$ plasmablasts (C) or IgA^+ $\alpha4\beta7^-$ plasmablasts (D) among $CD27^+CD38^+$ plasmablasts. (**E**) Table and forest plot of results for each B cell subpopulation on D8 and estimates of the difference between placebo and VXA-G1.1-NN with 95% confidence intervals are shown. Data are from N = 65 and N = 76 for the placebo and VXA-G1.1-NN study groups, respectively. Data in (B to D) are presented on each study day for VXA-G1.1-NN and placebo study groups as boxplots, with bounds from 25th to 75th percentile, median line, and whiskers, which extend to the largest or smallest value no further than 1.5 * the interquartile range. Points correspond to a sample from each participant. P-values, estimates, and significance were calculated with a linear mixed-effects model fitting each B cell parameter as the outcome and time, study group, and their interaction as main effects. Participant ID was fitted as a random effect. ****$p < 0.0001$; ns, not significant. (**F**) Heatmap of Spearman's correlation coefficient between log10 fold changes of B cell populations (D8/D1) and log10 fold changes of serum and mucosal antibody responses (D28/D1). Statistical significance is shown, *$p < 0.05$; **$p < 0.01$; ***$p < 0.001$; ns, not significant.

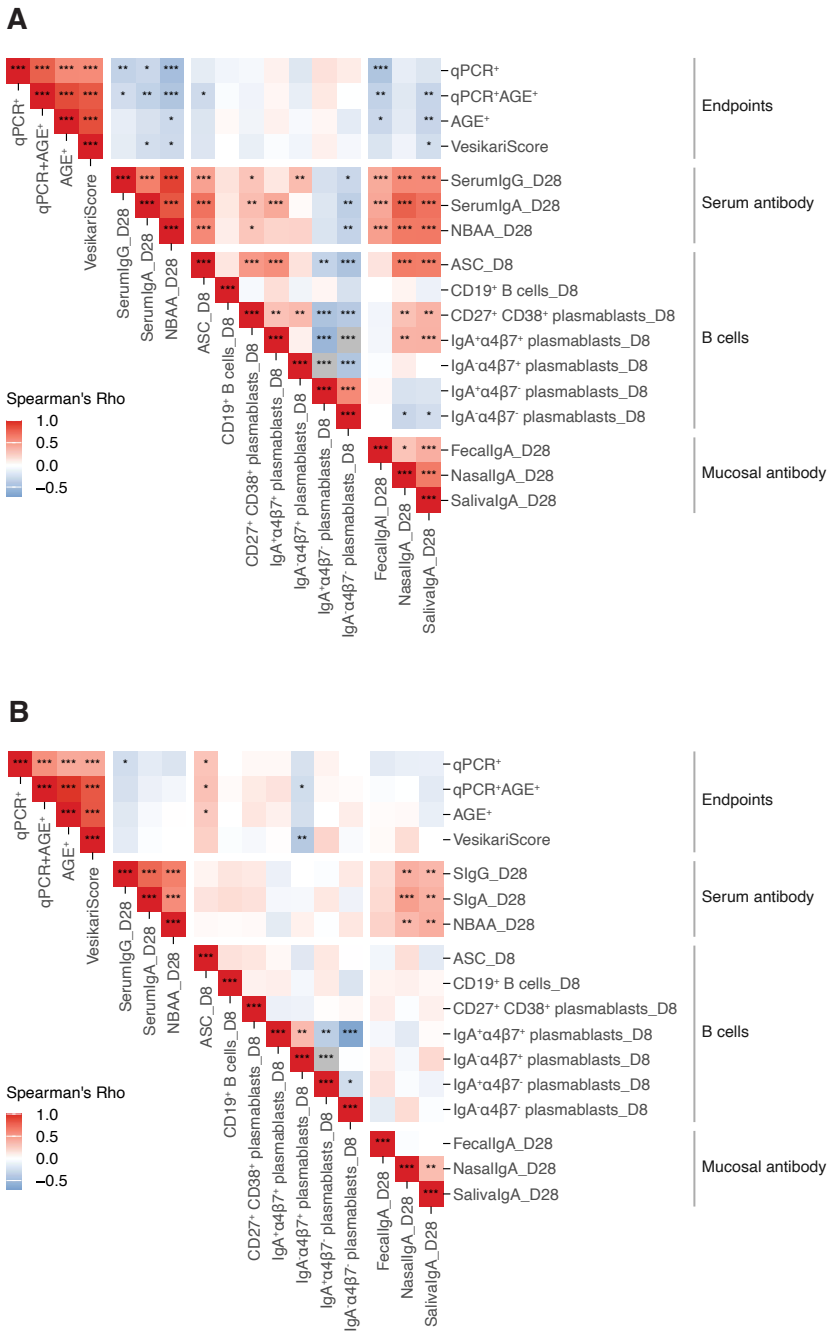

Figure S5. Correlations of pre-challenge serum or mucosal antibody concentrations and B cell frequencies with norovirus infection. (**A and B**) Heatmaps representing Spearman correlations between pairs of pre-challenge immune variables and infection or disease endpoints. Data are shown for the VXA-G1.1-NN (A, N = 76) and the placebo (B, N = 65) study groups. Variables are grouped into categories on the right margin: Serum antibody (serum IgG, IgA, and NBAA values measured on D28 post-vaccination); B cell frequencies (ASCs, total $CD19^+$ B cells, $CD27^+CD38^+$ plasmablasts, and plasmablasts expressing IgA or $a4\beta7^+$); mucosal antibody (IgA in fecal, nasal, or saliva samples); and endpoints (NV infection ($qPCR^+$), NV gastroenteritis ($qPCR^+AGE^+$), acute gastroenteritis (AGE^+), and gastroenteritis severity (Vesikari)). Statistical significance of each pairwise correlation is shown as $*p < 0.05$; $**p < 0.01$; $***p < 0.001$.

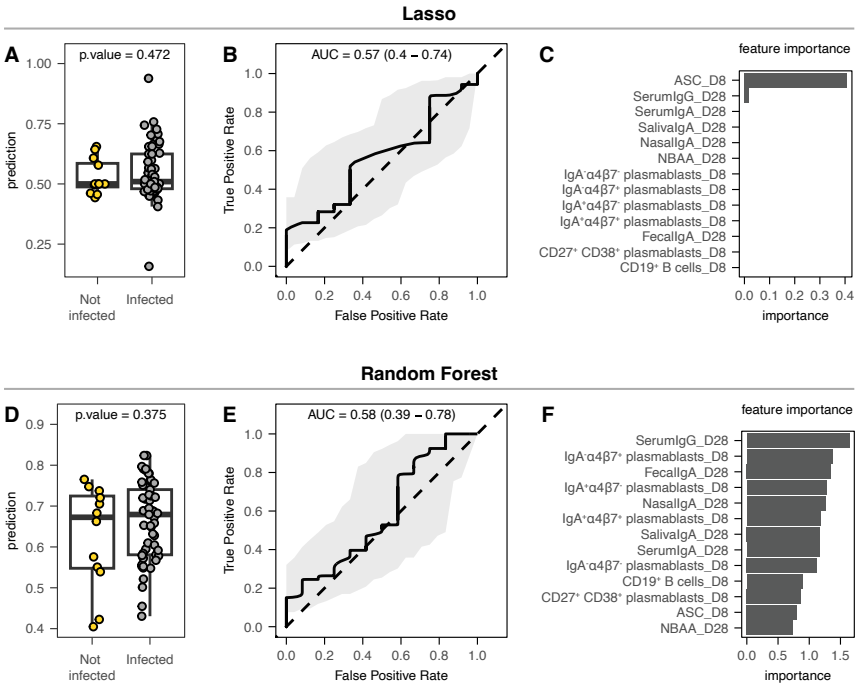

Figure S6. Lasso and random forest models do not predict infection in the placebo study group. Lasso and Random Forest prediction models were trained to predict whether a participant was infected or not using pre-challenge immunogenicity data collected twenty-eight days after placebo vaccination. Infection was defined as the detection of NV RNA in at least one stool or emesis sample during the study period. (**A to C**) Results of the Lasso model are shown. (**A**) Prediction scores are shown for N = 65 participants in the placebo study group with the true outcome, infected (N = 53) or not infected (N = 12) (Related to fig. S1A). (**B**) Prediction accuracy is shown with a receiver operating characteristic (ROC) curve and corresponding area under the curve (AUC) with 95% confidence intervals. (**C**) Pre-challenge immunogenicity features are shown with the corresponding importance score for model predictions. (**D to F**) Results of the Random Forest model are shown as in (A to C), including prediction scores (D), ROC curve and AUC (E), and feature importance scores (F). Data in (A) and (D) are presented as boxplots, with bounds from 25th to 75th percentile, median line, and whiskers, which extend to the largest or smallest value no further than 1.5 * the interquartile range. Points correspond to a model prediction of each participant. Prediction scores between infection classes was compared with a two-tailed Wilcoxon test and nominal p-values are shown within the plot.

Table S1. Baseline characteristics.

Analysis population	Vaccine phase (N = 165)		Challenge phase (N = 141)	
Study group	VXA-G1.1-NN	Placebo	VXA-G1.1-NN	Placebo
Number of participants, n	86	79	76	65
Age, years[a]	36 ± 8	34 ± 7	36 ± 8	35 ± 7
Male, n (%)	43 (50.0)	48 (60.8)	39 (51.3)	41 (63.1)
Body mass index, kg/m^2 [1]	27.1 ± 3.7	27.2 ± 3.9	26.9 ± 3.6	27.1 ± 3.9
Race, n (%)				
White	54 (62.8)	54 (58.4)	48 (63.2)	42 (64.6)
Black/African-American	21 (24.4)	14 (17.7)	19 (25.0)	13 (20.0)
Asian	5 (5.8)	8 (10.1)	5 (6.6)	7 (10.8)
American Indian or Alaskan Native	1 (1.2)	0	1 (1.3)	0
Multi-Racial	5 (5.8)	3 (3.8)	3 (3.9)	3 (4.6)
Ethnicity, n (%)				
Latino or Hispanic	37 (43.0)	33 (41.8)	32 (42.1)	26 (40.0)
Not Latino or Hispanic	49 (57.0)	46 (58.2)	44 (57.9)	39 (60.0)

[1]mean ± standard deviation

Table S2. Solicited symptoms of reactogenicity for Day 1 through Day 8 post-vaccination and solicited NV symptoms post-challenge.

	VXA-G1.1-NN N (%)	Placebo N (%)
VACCINE PHASE, $N_{(V)}$=165[1]	**$N_{(v)}$=86**	**$N_{(v)}$=79**
Participants reporting ≥ 1 solicited symptoms (Day 1 - Day 8)	50 (58.1)	36 (45.6)
Maximum severity mild	38 (44.2)	31 (39.2)
Maximum severity moderate	12 (14.0)	5 (6.3)
Maximum severity severe	0 (0.0)	0 (0.0)
Malaise/Fatigue	25 (29.1)	20 (25.3)
Myalgia	11 (12.8)	12 (15.2)
Anorexia	10 (11.6)	6 (7.6)
Headache	25 (29.1)	19 (24.1)
Fever	0 (0.0)	0 (0.0)
Diarrhea	20 (23.3)	12 (15.2)
Nausea	13 (15.1)	10 (12.7)
Vomiting	0 (0.0)	1 (1.3)
Abdominal Pain	14 (16.3)	8 (10.1)
CHALLENGE PHASE, $N_{(C)}$=141[2]	**$N_{(c)}$=76**	**$N_{(c)}$=65**
Participants reporting ≥ 1 solicited norovirus symptoms post challenge	59 (77.6)	55 (84.6)
Maximum severity mild	25 (32.9)	22 (33.8)
Maximum severity moderate	25 (32.9)	21 (32.3)
Maximum severity severe	9 (11.8)	12 (18.5)
Fever	4 (5.3)	4 (6.2)
Nausea	38 (50.0)	38 (58.5)
Vomiting	28 (36.8)	33 (50.8)
Diarrhea	21 (27.6)	15 (23.1)
Myalgia	36 (47.4)	31 (47.7)
Abdominal cramps or pain	32 (42.1)	39 (60.0)
Abdominal gurgling or bloating	46 (60.5)	39 (60.0)

[1] $N_{(V)}$ number of participants vaccinated; $N_{(C)}$ number of participants challenged
[2] $N_{(C)}$ number of participants challenged

Table S3. Unsolicited adverse events (UAE) from D1 through C29 by study phase.

	VXA-G1.1-NN n (%)	Placebo n (%)
Serious adverse events[1] (Day 1 – Day C29)	0 (0.0)	0 (0.0)
VACCINE PHASE (n=165)	**$N_{(v)}$=86**	**$N_{(v)}$=79**
Number of participants reporting ≥ 1 UAE during vaccination phase, $n_{(v)}$=165 [2]	7 (8.1)	9 (11.4)
Participants with ≥ 1 UAE related to vaccination	3 (3.5)	3 (3.8)
Gastrointestinal disorders		
Anal Fissure	1 (1.2)	0 (0.0)
Constipation	0 (0.0)	2 (2.5)
Diarrhea	1 (1.2)	0 (0.0)
Nausea	0 (0.0)	1 (1.3)
General disorders and administration site conditions		
Fatigue	1 (1.2)	1 (1.3)
Malaise	1 (1.2)	0 (0.0)
Infections & Infestations		
COVID-19	2 (2.3)	2 (2.5)
Sinusitis	1 (1.2)	0 (0.0)
Viral upper respiratory infection	1 (1.2)	0 (0.0)
Metabolism and nutrition disorders		
Decreased appetite	1 (1.2)	1 (1.3)
Musculoskeletal and connective tissue disorders		
Back Pain	0 (0.0)	1 (1.3)
Nervous system disorders		
Headache	0 (0.0)	2 (2.5)
Syncope	1 (1.2)	0 (0.0)
Respiratory, thoracic and mediastinal disorders		
Cough	0 (0.0)	1 (1.3)
Skin and subcutaneous tissue disorders		
Pruritis	1 (1.2)	0 (0.0)
CHALLENGE PHASE (n=141)	**$N_{(c)}$=76**	**$N_{(c)}$=65**
Number of participants reporting ≥ 1 UAE during challenge phase, $n_{(c)}$=141[2]	31 (40.8)	23 (35.4)
Participants with ≥ 1 UAE related to challenge	16 (21.1)	15 (23.1)
Cardiac Disorders		
Tachycardia	1 (1.3)	0 (0.0)
Gastrointestinal disorders		
Diarrhea	1 (1.3)	0 (0.0)
Gastroesophageal reflux disease	1 (1.3)	0 (0.0)
General disorders and administration site conditions		
Chills	3 (3.9)	2 (3.1)
Infections & Infestations		
Bacterial vaginosis	1 (1.3)	0 (0.0)
COVID-19	1 (1.3)	1 (1.5)
Groin abscess	0 (0.0)	1 (1.5)
Hordeolum	1 (1.3)	0 (0.0)
Upper respiratory tract infection	0 (0.0)	1 (1.5)
Viral upper respiratory tract infection	1 (1.3)	0 (0.0)
Injury, poisoning and procedural complications		
Skin laceration	0 (0.0)	1 (1.5)
Musculoskeletal and connective tissue disorders		
Back pain	1 (1.3)	2 (3.1)
Flank pain	1 (1.3)	0 (0.0)
Muscle spasms	0 (0.0)	1 (1.5)
Neck pain	1 (1.3)	0 (0.0)
Nervous system disorders		
Dizziness	0 (0.0)	1 (1.5)
Headache	20 (26.3)	16 (24.6)
Reproductive system and breast disorders		
Dysmenorrhea	1 (1.3)	1 (1.5)
Respiratory, thoracic and mediastinal disorders		
Throat irritation	1 (1.3)	0 (0.0)
Skin and subcutaneous tissue disorders		
Rash	0 (0.0)	1 (1.5)

[1] Not included in this table are the 2 reported events during safety FU phase: 1 placebo participant reported 2 SAEs: leg cellulitis and deep vein thrombosis (DVT) following skin laceration, unrelated to vaccine or challenge.

[2] $n_{(v)}$ number of participants vaccinated; $n_{(c)}$ number of participants challenged

Table S4. Antibody responses at D1 (baseline), D28, or C29 following oral vaccination.

	VXA-G1.1-NN	Placebo
Serum NBAA titer		
Day 1 (baseline), n	75	65
Geometric mean titer (95% CI)	33.29 (25.9 - 42.8)	31.61 (25.02 - 39.93)
Day 28, n	76	65
Geometric mean titer (95% CI)	132.07 (99.45 - 175.38)	32.29 (25.36 - 41.12)
Day 57, n	76	64
Geometric mean concentration (95% CI)	848.86 (600.35 - 1200.24)	925.95 (610.93 - 1403.42)
Serum Anti-VPI G1.1 IgA (AU/mL)		
Day 1 (baseline), n	76	65
Geometric mean concentration (95% CI)	889112.99 (602308.11 - 1312487.59)	714918.55 (493724.06 - 1035210.91)
Day 28, n	76	65
Geometric mean concentration (95% CI)	6415804.23 (4388487.42 - 9379665.47)	732526.94 (506386.12 - 1059657.23)
Day 57, n	76	64
Geometric mean concentration (95% CI)	19082415.31 (13697577.35 - 26584158.98)	25759340.6 (16745791.62 - 39624500.48)
Serum Anti-VPI G1.1 IgG (AU/mL)		
Day 1 (baseline), n	76	65
Geometric mean concentration (95% CI)	969388.84 (720754.47 - 1303793.13)	790885.47 (588504.54 - 1062863.22)
Day 28, n	76	65
Geometric mean concentration (95% CI)	4506406.63 (3246347.48 - 6255553.63)	793556.71 (590696.9 - 1066083.57)
Day 57, n	76	64
Geometric mean concentration (95% CI)	21546128.47 (15688823.68 - 29590214.12)	22930396.48 (15476375.69 - 33974561.83)
Fecal IgA (units)		
Day 1 (baseline), n	76	65
Geometric mean titer (95% CI)	715.61 (442.64 - 1156.92)	470.86 (316.78 - 699.89)
Day 28, n	76	65
Geometric mean titer (95% CI)	1888.5 (1221.07 - 2920.74)	444.31 (304.83 - 647.6)
Day 57, n	75	63
Geometric mean concentration (95% CI)	6122.41 (3891.96 - 9631.1)	5047.08 (3000.21 - 8490.39)
Nasal Anti-VP1 GI.1 IgA (RLU/µg Total IgA)		
Day 1 (baseline), n	76	65
Geometric mean concentration (95% CI)	48.4 (39.1 - 59.91)	40.61 (32.99 - 50)
Day 28, n	76	65
Geometric mean concentration (95% CI)	175.41 (132.89 - 231.52)	40.61 (32.81 - 50.26)
Day 57, n	76	64
Geometric mean concentration (95% CI)	244.88 (196.01 - 305.93)	264.09 (200.6 - 347.69)
Saliva IgA		
Day 1 (baseline), n	76	65
Geometric mean concentration (95% CI)	0.4 (0.31 - 0.51)	0.31 (0.27 - 0.35)
Day 28, n	76	65
Geometric mean concentration (95% CI)	1.15 (0.84 - 1.57)	0.35 (0.31 - 0.4)
Day 57, n	76	64
Geometric mean concentration (95% CI)	1.81 (1.33 - 2.44)	1.84 (1.41 - 2.4)

Table S5. Norovirus GI.1 Primers and Probes.

Name	Detection	Sequence (5' – 3')
COG 1F mod	Norovirus GI Forward Primer	CGY TGG ATG CGI TTY CAT GA
COG 1R	Norovirus GI Reverse Primer	CTT AGA CGC CAT CAT CAT TYA C
Ring 1E	Norovirus GI Probe	FAM- TGG ACA GGR GAY CGC-MGBNFQ
MS2F	MS2 Forward Primer	TGG CAC TAC CCC TCT CCG TAT TCA CG
MS2R	MS2 Reverse Primer	GTA CGG GCC ACC CCA CGA TGA C
MS2 Probe	MS2 Probe	HEX-CAC ATC GAT AGA TCA AGG TGC CTA CAA GC-BHQ-1

Table S6. Antigens and fluorophores used for staining.

Antigen	Fluorophore	Vendor	Catalog Number
CD19	SB780	Invitrogen	78-0199-41
CD38	PerCP-eFluor 710	Invitrogen	46-0389-42
CD27	PE-Cy7	BD Biosciences	46-0389-42
Integrin β7	PE	BD Biosciences	555945
IgD	eFluor 506	Invitrogen	69-9868-42
IgA	FITC	Invitrogen	A24459

Data file S1. Individual-level data